

NATIONAL TRANSPORTATION SAFETY BOARD

Office of Research and Engineering
Washington, D.C. 20594

November 9, 2010

Hover Study Addendum #2

by John O'Callaghan

A. ACCIDENT

Location: Weaverville, CA

Date: August 5, 2008

Time: 19:41 Pacific Daylight Time (PDT)¹

Aircraft: Sikorsky S-61N helicopter, registration N612AZ

NTSB#: LAX08PA259

B. GROUP

Not Applicable

C. HISTORY OF FLIGHT

On August 5, 2008, about 1941 Pacific daylight time, a Sikorsky S-61N helicopter, N612AZ, impacted trees and terrain during the initial climb after takeoff from Helispot 44, located at an elevation of about 6,000 feet in mountainous terrain near Weaverville, California. The airline transport pilot, the safety crewmember and seven firefighters were killed; the commercial copilot and three firefighters were seriously injured.² Impact forces and a postcrash fire destroyed the helicopter. The helicopter was being operated by the United States Forest Service (USFS) as a public flight to transport the firefighters from Helispot 44 to another location. The helicopter was registered to Carson Helicopters, Inc. (CHI) of Grants Pass, Oregon, and leased to Carson Helicopter Services, Inc. (CHSI) of Grants Pass. The USFS had contracted with CHI for the services of the helicopter.³ Visual meteorological conditions prevailed at the time of the accident, and a company visual flight rules flight plan had been filed.

The Hover Study for this accident (Reference 1) presents the results of computing the maximum weight at which the helicopter could hover out-of-ground-effect (HOGE) as a function of time for the seven takeoffs recorded on the helicopter's Cockpit Voice Recorder (CVR). The calculations are based on:

¹ Local time at Weaverville on the day of the accident was Pacific Daylight Time (PDT). PDT = UTC - 7 hours. Times in this Study are in PDT unless otherwise noted.

² The safety crewmember was a USFS Inspector Pilot.

³ Initially, the NTSB was informed that the contract was between the USFS and CHSI. For further information refer to the Operations Factual Report.

- The gas-generator speed (N_g) of the two engines obtained from a sound-spectrum analysis of the engine sounds recorded on the CVR.
- The shaft horsepower required to HOGE as a function of helicopter weight and atmospheric conditions, as provided by the appropriate performance chart in the CHI Rotorcraft Flight Manual Supplement #8 (RFMS #8).
- The shaft horsepower (SHP) provided by each engine as a function of N_g , as generated by General Electric (GE) (the engine manufacturer) using mathematical models of the engines' performance.
- Helicopter gross weight values provided by the Operations Group.

The results of the calculations indicate that on the accident takeoff from Helispot 44 (H44), the helicopter was operating within 100 lb. of the HOGE weight corresponding to the shaft horsepower generated by the engines at their maximum ("topping") N_g . The results also indicate that the helicopter was operating under similar but slightly less critical conditions during two previous (successful) takeoffs from H44.

Addendum #1 to the Hover Study (Reference 2) presents calculations of the torque developed by the engines during the accident takeoff, based on:

- The main rotor speed (N_R) obtained from a sound-spectrum analysis of the planetary mesh sounds recorded on the CVR, as described in the *Sound Spectrum Study Cockpit Voice Recorder* (Reference 3) and presented in the Hover Study.
- The gas-generator speed (N_g) of the two engines obtained from a sound-spectrum analysis of the engine sounds recorded on the CVR, as described in Reference 3 and presented in the Hover Study.
- The shaft horsepower (SHP) provided by each engine as a function of N_g , as generated by General Electric (GE) (the engine manufacturer) using mathematical models of the engines' performance and presented in the Hover Study.
- The physical relationship between power, torque, and main rotor speed, by which torque can be computed from shaft horsepower and N_R .

The calculations in Addendum # 1 are presented as plots of N_R and torque vs. time, with relevant comments from the CVR indicated on the plots at positions corresponding to the times at which they were recorded. The plots indicate that the torque and N_R callouts by the crew during the accident takeoff are consistent with the N_R values based on the CVR sound spectrum analysis, and with the torque calculations presented in Addendum #1. This in turn indicates that the power developed by the engines during the accident takeoff matched the power expected based on the N_g values determined from the sound spectrum analysis, and the mathematical models of the engines' performance provided by GE.

This second Addendum to the Hover Study presents the results of simulations of the accident takeoff performed by Sikorsky Aircraft Company (SAC) using the GenHel helicopter simulation computer program. The program uses the N_R obtained from Reference 3, as well as the approximate time from liftoff to impact with the trees as determined from the CVR transcript (Reference 4), to compute the flight path of the helicopter during the accident takeoff, for each of the following power-required conditions:

- Power required performance at an outside air temperature (OAT) of 23° C, as defined in the CHI Rotorcraft Flight Manual Supplement (RFMS) #8;
- Power required performance at an OAT of 20° C, as defined in the CHI RFMS #8;
- Power required performance at an OAT of 23 C°, based on SAC / United States Navy (USN) flight tests of a USN NVH-3A helicopter equipped with CHI composite main rotor blades (CMRB), and on SAC / CHI flight tests of a CHI S-61A helicopter equipped with CHI CMRB;
- Power required performance at an OAT of 20° C, based on the flight tests of the USN NVH-3A and CHI S-61A helicopters with CMRB.

All simulations use a helicopter gross weight of 19,008 lb. and calm winds. For these simulations, the torque applied to the main rotor during the period of time that the engines are at topping and the N_R is decreasing is based on a refinement of the torque calculation presented in Reference 2. In Reference 2, the horsepower produced by the engines at topping N_G and 103% N_R is used to compute torque at all the points where the engines are at topping, even those where N_R decreases below 103%. In the GenHel simulations, the decrease in engine power at topping as N_R decreases (resulting from a reduction in engine efficiency) is accounted for in the torque calculation, resulting in torque values during the N_R decay that are smaller than those presented in Reference 2.

The tree that was first struck by the accident helicopter was about 55 ft. high⁴, and 195 ft from the departure point of the helicopter (see Reference 7). The results of the simulations indicate that the helicopter will clear this tree if the power required performance based on RFMS #8 is used, but will not clear the tree if the power required performance based on the SAC / USN flight tests is used.

The sections that follow describe the GenHel simulation in general, and specific adjustments made to the simulation models to reflect both the CHI RFMS #8 and the SAC / USN flight test performance, and to account for the performance effects of an underbelly water tank (the “Fire King” tank) installed on the accident helicopter. The results of the simulations are then presented in greater detail.

The methods used to conduct hover performance flight tests at SAC are briefly described, as well as a comparison of the recent USN / SAC / CHI flight test results with independent tests conducted by Whipple Aviation Services on behalf of CHI in 2009. These test results are also compared with the flight test data that forms the basis of CHI RFMS #8. The HOGE weights determined from each of these data sets, and accounting for the performance effects of the Fire King tank, are also presented.

Appendix A contains a copy of SAC’s report detailing the computation of the download forces and aerodynamic drag on the Fire King tank. The results of these calculations were incorporated into the GenHel simulation models.

⁴ The tree height information was provided to the author through a conversation with the Airworthiness Group Chairman. The measured height of the main rotor blade contact point on the tree was 49.5 feet.

D. DETAILS OF THE INVESTIGATION

I. Simulation Overview

This section provides a brief description of helicopter simulation in general, and then describes the implementation of the GenHel S-61N simulation for the USFS accident in particular.

The simulations described in this Addendum are special applications of the SAC GenHel S-61N engineering simulator.⁵ The ways these special cases work are best understood in terms of how they differ from a “standard” simulation, in which a human pilot seated at the controls of a simulator cab (a mockup of an actual helicopter cockpit) makes control inputs as he would in a real helicopter, and the simulation calculates the appropriate response in the control forces, helicopter motion, instrument displays, and visual scene.

Figure 1 is a flow chart describing the logic and data flow in a standard simulation.⁶ The boxes with bold lines and non-italicized text represent simulation models, that is, units of computer code and data that describe the behavior of a part of the helicopter or its systems mathematically. The boxes with non-bold lines and italicized text represent physical quantities or values computed by the simulation models. The arrows indicate which simulator models compute the various physical quantities, and how these quantities are in turn used as inputs by other models.

The two gray boxes in Figure 1 labeled “Main Rotor Module” and “Tail Rotor Module” represent sets of more complex models and data needed to compute the physical behavior of the main and tail rotor systems. These modules can be thought of as simulations within the simulation, in that the motion of the main rotor and tail rotor blades are themselves determined by computing the forces and moments acting on the blades, and then solving the governing equations of motion (see Figure 2).⁷ The main rotor and tail rotor local equations of motion consider both aerodynamic and inertial loads on the blades, and account for the velocities and accelerations at the hubs. The need to solve for the dynamic response of the main and tail rotors is one of the factors that makes helicopter simulations more complex than fixed-wing airplane simulations.

Starting with the box labeled “Human Pilot” in Figure 1, we see that by manipulating the simulator cab controls the pilot can generate inputs to the collective, longitudinal and lateral cyclic, tail rotor pedals, throttles, landing gear lever, and other cockpit controls duplicated in the cab. He can also provide inputs to the Flight Management Computer and Flight Director (which also acts as an autopilot). In the case of “desktop” engineering simulations, which run on the computer without a cab, these “pilot” inputs are accomplished by computer code. For both desktop and cab-based simulations, the pilot inputs are eventually processed by the simulator flight controls model that calculates the appropriate response of the main rotor collective and cyclic pitch angles and the tail rotor collective pitch angle. The Stability

⁵ References 5 and 6 contain detailed descriptions of the mathematical models underlying the GenHel simulation. These References were written specifically to document the implementation of a GenHel simulation of the UH-60A BlackHawk helicopter, and not an S-61; however, the mathematical models that are the foundation of both simulations are the same.

⁶ Figure 1 does not represent either the specific data flow or the architecture of the SAC GenHel model, and is used here for explanatory purposes only.

⁷ Figure 2 does not represent either the specific data flow or the architecture of the SAC GenHel model, and is used here for explanatory purposes only.

Augmentation System (SAS) model computes additional main rotor and tail rotor blade inputs, based on the helicopter's motion state variables and SAS control laws, to stabilize the helicopter.

The S-61 does not have a throttle in the conventional sense, but uses speed control levers to set the desired rotational speed for the main rotor. A separate fuel control on each engine acts as a governor to maintain that speed. The SAS provides stabilizing inputs that are added mechanically to the pilot's stick commands, in the closed loop control system.

On an actual helicopter, the control system makes inputs via mechanical linkages to hydraulic servos that position the rotor swashplate as required to obtain the desired collective and cyclic pitch angles on the blades. The GenHel S-61 simulation does not model this linkage, actuator, swashplate, and blade angle geometry explicitly; rather, it uses a mathematical transformation to relate cockpit control inputs to collective and cyclic pitch blade angles directly.

The main rotor collective and cyclic pitch blade angles are used by the main rotor module, along with the motion state variables and variables describing the wind, atmospheric properties, and the driving torque about the main rotor shaft provided by the engines, to compute the dynamic response of the rotor and the forces and moments it imposes on the helicopter fuselage through the rotor hub. As shown in Figure 2 and mentioned above, the main rotor module is a "simulation within a simulation:" the forces and moments on the blades are computed, and then the equations that govern their motion are solved to update the variables that describe the state of the rotor. These variables include the rotor RPM, flapping angles, lead-lag angles, and the local speed, dynamic pressure, Mach number, inflow angles and angles of attack and sideslip along each blade. Since many state variables can vary greatly over different parts of the rotor disk, the forces and moments on the blades are computed by dividing each blade into segments along the span, computing the local lift, drag, and moment contributions of each segment, and then summing the contributions of all the segments.

The main rotor module contains a "rotor air mass degree of freedom" that represents the inflow angles over the rotor, and the orientation of the rotor wake as it leaves the rotor (which affects the local flow over the fuselage and vertical and horizontal stabilizers). As described in Reference 5, the downwash distribution over the rotor is computed based on the rotor loading, which is determined from momentum considerations and includes a "basic momentum component which results from generating aerodynamic rotor thrust," "a harmonic momentum component which derives from cyclic aerodynamic hub moments on the rotor disk," and "a harmonic component due to rotor wake blow-back with increasing forward speed."⁸

In addition to the forces and moments at the rotor hub, the output of the main rotor module includes rotor wake information that is used in computing the local flow angles and dynamic pressures over other helicopter components, such as the fuselage, the vertical stabilizer, and the horizontal stabilizer, and tail rotor. The local flow properties are used by the aerodynamic models of these sub-components to compute their contributions to the forces and moments about the helicopter's center of gravity.

In the GenHel model, air flow velocities on each rotor blade element are composed of those due to the motion of the helicopter, those due to the motion of the blades in flapping and lagging, those due to external influences like wind and gusts, and those due to the production

⁸ Reference 5, p. 13-14.

of lift (induced velocities). A separate sub-module calculates the induced velocities on each blade element based on rotor thrust and advance ratio. Rotor downwash velocities on the fuselage and empennage are calculated using table lookups of the portion of rotor induced velocity that is to be applied at the location of interest. These look-up tables are based on vortex wake theory, but modified empirically to better match actual SAC flight test data.

The torque about the rotor shaft produced by the aerodynamic forces on the rotor blades is used by the engine model to compute the response of the engines as they attempt to maintain the target rotor RPM. The sum of these torques, and the rotor inertia, are used to compute the rotor angular acceleration and velocity. For the simulation used in this investigation, N_R is driven directly using the CVR-based N_R , and so it is not necessary to compute N_R . However, the CVR-based N_R is used with simulation models to determine the proportion of engine torque consumed by the tail rotor and other helicopter systems, and the remaining torque available to drive the main rotor. This remaining torque serves as an *a-priori* target for setting the collective angle in the simulation.

The sum of all the forces and moments on the helicopter's fuselage are used along with quantities calculated by the mass properties model in the solution of the equations of motion that determine the motion states, both angular and linear.⁹ Angular states are the helicopter's yaw, pitch and roll angles, and their time derivatives (angular rates and accelerations). Linear states are the components of the three dimensional position of the helicopter in space and their time derivatives (velocities and accelerations). These states are also used as inputs to the various mathematical models that compute the quantities that eventually affect the forces and moments.

In the case of cab-based simulations, information about the helicopter motion states and from the propulsion model are used to drive the visual displays and cockpit instruments in the cab. For simulator cabs on a motion base, the motion information can be used to maneuver the base in an attempt to duplicate, within limits, the acceleration cues felt by the pilots.

GenHel "Desktop" Simulation Customizations for USFS Accident

The simulations of the USFS accident using SAC's GenHel "desktop" simulation differ from the "standard" simulation just described in several ways. For all scenarios, the main rotor RPM is driven directly with data prepared *a priori*, as opposed to calculating them within the simulation itself,¹⁰ and the longitudinal and lateral cyclic flight controls are driven as required to fly the helicopter from the departure point to the first tree strike in a time consistent with that recorded on the CVR.

The N_R , N_g , computed power, and computed hover-out-of-ground-effect (HOGE) weight for the accident takeoff is shown in Figure 10a of the Hover Study, duplicated here as Figure 3. This Figure shows that the N_g on each engine reached its maximum (topping) value of 101.5%-102% at about 19:41:08, and that the CVR-based data ends at about 19:41:39, shortly after the helicopter impacted trees. Assuming that at the time that the engines reached topping, the helicopter was still over the departure point but had started to move towards the

⁹ For the simulations performed in this investigation, the mass properties of the helicopter (weight, CG, and inertias) were kept constant for the short simulation times of interest.

¹⁰ However, as described above, the CVR-based N_R is used with the simulation models to determine the torque available to drive the main rotor, which in turn is used to drive the collective angle.

trees, then the CVR indicates that it took about 30 seconds to fly from the departure point to the location of the first tree strike. In the GenHel simulations, the cyclic controls are manipulated so as to fly the helicopter towards the trees in a way that duplicates this timing.

Another modification of the GenHel simulation used in this investigation involves customizing the rotor model to duplicate the HOGE weight at topping power specified in both the CHI RFMS #8, and SAC's prediction of the S-61N performance with CMRBs. SAC's prediction of the S-61N performance is based on the flight tests of the USN NVH-3A with CHI CMRBs, adjusted as required to account for configuration differences between the NVH-3A and S-61N. In GenHel, the target HOGE performance is matched by adjusting two parameters in the rotor model: the rotor blade skin friction drag, and the rotor "radial skew factor," which adjusts the distribution of rotor downwash along the rotor span. The proper GenHel performance level was confirmed by noting that GenHel reproduced the same HOGE performance as RFMS #8 and the SAC prediction for the S-61N with CHI CMRBs, for the accident conditions shown in Table 1. The flight tests are discussed further in Section D-II.

The GenHel models are further modified to account for an additional 103 lb. download force and additional aerodynamic drag acting on the "Fire King" tank installed under the belly of the accident helicopter.¹¹ Appendix A presents SAC's calculations of the download and drag increments resulting from the Fire King tank.

Finally, the rotor collective angle in the GenHel simulation is controlled so as to achieve a pre-determined torque target for the main rotor. This torque target is derived from the total torque produced by the engines, and an estimate of the proportion of engine torque consumed by the tail rotor and other helicopter systems. Specifically, the engine N_G and main rotor N_R speeds determined from the CVR are used in the General Electric mathematical model of the engines to derive the total engine torque. During the period that the engines are at topping and N_R is decreasing, this torque is slightly less than the torque presented in Reference 2, because unlike in Reference 2, the decrease in engine power at topping as N_R decreases (resulting from a reduction in engine efficiency) is accounted for. Figures 4a and 4b compare the total engine power and torque used in the GenHel simulations with the power and torque presented in Reference 2. Only a portion of the total engine torque is available to drive the main rotor, because of the power demands of the tail rotor and other helicopter systems. These demands are estimated *a priori* using models of these systems.

The resulting main rotor torque target and other simulation results are presented and discussed in Section D-III.

HOGE weight at 6106 ft., lbs. No Fire King tank installed		
Source	Temperature	
	20° C	23° C
CHI-1000-1 report (RFMS #8)	19333	19120
SAC S-61N 2010 prediction	18753	18545

Table 1. HOGE weights at 6106 ft. pressure altitude and 20° C and 23° C based on CHI RFMS #8 data and SAC's 2010 prediction of the S-61N performance with CHI CMRBs.

¹¹ The "Fire King" tank carries up to 900 gallons of water for the aerial suppression of forest fires. The dimensions of the tank were provided by CHI to the NTSB. The NTSB forwarded these dimensions to SAC, who computed the download and aerodynamic drag effects. SAC's calculations are presented in Appendix A.

II. Flight tests of USN NVH-3A and CHI S-61A helicopters with Carson / Ducommun Composite Main Rotor Blades

This section provides an overview of SAC's techniques for HOGE flight testing in general (i.e., not particular to any specific helicopter), and provides a limited description of relevant HOGE flight tests of both a USN NVH-3A helicopter and CHI S-61A helicopter equipped with Carson / Ducommun CMRBs (the same type of blades installed on the accident helicopter). In addition, relevant results of a separate flight test sponsored by CHI using a S-61N equipped with CHI CMRBs are presented.

Hover performance flight testing at the Sikorsky Aircraft Company

At the request of the NTSB, SAC provided¹² the following description of the methods used at the company to measure the hover performance of a helicopter:

Hover performance testing is performed to measure power required to hover. Key parameters are power, which is usually derived from the engines' torque meters and main rotor or power turbine speed, aircraft gross weight, which is determined by subtracting fuel burn from aircraft takeoff gross weight, main rotor speed, ambient air temperature and pressure, wind speed and direction and aircraft height above ground. Aircraft parameters are usually recorded on an onboard data system. This allows the data to be examined after the flight to ensure steady state data was recorded.

Testing is usually performed out of ground effect and at several lower wheel heights to determine the ground effect benefit.

Testing is also performed over a range of referred rotor speeds (rotor speed / square root of temperature ratio). Hover performance can vary with referred rotor speed which is a measure of rotor tip Mach number.

Power can also be independently determined from main and tail rotor power derived from strain gages on the main rotor shaft and tail rotor drive shaft and their rotational speeds and an estimate of other power losses (generators, hydraulic pumps, oil cooler blower etc.) Special care is also taken to calibrate the engine torque meters or obtain engine test cell torque meter calibration data for the test engines.

It is important to accurately know aircraft start gross weight. For this type of test we typically do pre- and post- flight roll-on weighings of the aircraft. The difference between these two is used to verify the fuel burned measurements or fuel quantity indications.

Relative wind speed and direction can have a large impact on hover power required. We conduct hover performance testing only in winds of 3 kts or less. It is also important to know the wind speed and direction at the aircraft altitude. For OGE (~100 ft wheel height) hover performance testing we deploy a weather balloon with anemometer packages attached to its tether line. The balloon is deployed to a height so the anemometer is at the aircraft altitude. On many test days we have seen indications of calm winds on the ground (lake like a mirror) and winds of 5 kts or more at 100 ft. Streamers on the balloon tether line in the attached picture [Figure 5] illustrate this. To help confirm low winds at the test altitude, data points can be taken nose to wind, right side to wind, tail to wind and left side to wind.

For in ground effect data it is important to know the exact height of the aircraft above the ground. The closer the aircraft is to the ground the more critical this is. To verify radar altitude indications, a weighted rope of known length is attached to the main landing gear. The aircraft is then guided until the end of the rope is just touching the ground and the radar altitude indication noted.

For free flight hover performance testing, several flights are required to determine hover performance over a range of gross weights.

¹² This information was provided to the author in an email dated 8/24/2010.

A tethered hover test technique can also be used. This allows a large range of rotor thrust levels to be acquired without re-ballasting the aircraft. Here the aircraft is tethered to the ground and tether cable tension and cable angles are measured. Tether cable tension is measured and added to aircraft weight to determine main rotor thrust. The cable angles are displayed to the pilot so he can keep the tether cable vertical.

Data is typically presented as weight coefficient versus power coefficient for constant referred rotor speeds. Both weight coefficient and power coefficient have air density in the denominator. To obtain a broad enough range of data to cover the full hover capability of the aircraft, hover performance data usually also has to be taken at an altitude test site.

Important points to note in this description of how hover performance flight testing is conducted at SAC are that:

- Key performance parameters (power, fuel burn, N_R , air temperature and pressure, wind speed and direction, aircraft height above ground) are sensed and recorded with appropriate instrumentation, which allows precise post-flight processing of the data.
- Steady-state conditions (verified using recorded data) are to be used for hover performance calculations.
- Wind speeds of 3 knots or less are used for hover performance flight tests. Because low-wind conditions are so critical, test points at various helicopter headings are obtained (large scatter in the results at different headings would indicate non-negligible winds).
- Winds at altitude can differ from winds at the surface (see, for example, Figure 5). The wind at the test altitude is monitored using anemometer packages attached to the tether line of a weather balloon.

The weight coefficient¹³ and power coefficient referred to in the SAC flight test description are defined as follows:

$$C_T = \frac{T}{\rho A (\Omega r)^2} \quad [1]$$

$$C_P = \frac{P}{\rho A (\Omega r)^3} \quad [2]$$

Where:

T = rotor thrust (assumed to equal the helicopter weight)
 P = the total power produced by the helicopter's engines
 ρ = air density

¹³ In this Addendum, "weight coefficient" and "thrust coefficient" are used interchangeably, although the two are not strictly equivalent. The thrust produced by the rotor will have to be somewhat greater than the weight of the helicopter, since in addition to the helicopter weight, the rotor has to overcome aerodynamic download forces on the fuselage and other helicopter components resulting from the rotor wash.

A = rotor disk area
 Ω = rotor angular speed
 r = rotor radius

The “referred rotor speed” mentioned in the flight test description is defined as follows:

$$N_{Rref} = N_R \sqrt{\frac{t}{t_{std}}} \quad [3]$$

Where t is the air temperature, and t_{std} is the standard air temperature at sea level. t and t_{std} must be expressed in terms of absolute temperature, i.e., °Rankine or °Kelvin. The referred rotor speed accounts for Mach number effects on the rotor as the speed of sound is reduced at lower temperatures.

Results of flight tests of a USN NVH-3A and CHI S-61A equipped with CHI CMRBs

In 2008, SAC and the USN performed extensive hover performance flight tests with a USN NVH-3A helicopter equipped with CHI CMRBs. On the basis of the data collected during these tests, in 2010 SAC predicted the hover performance of the S-61A helicopter equipped with CHI CMRBs by applying performance increments and decrements as appropriate to account for the configuration differences between the NVH-3A and S-61A. In addition, SAC “spot checked” these calculations in cooperation with CHI, using a CHI-owned S-61A equipped with CHI CMRBs (N3173U).

The results of the flight tests with N3173U are documented by SAC in Reference 10, and by CHI in Reference 11. A plot of C_P vs. C_T derived from these tests, taken from Reference 10, is shown here as Figure 6. The red line on the plot shows SAC’s prediction of the S-61A performance based on the SAC / USN testing of the NVH-3A.

The test results exhibit considerable data scatter at the higher thrust levels, which SAC attributes to wind effects at the test altitude. The hover tests were conducted with the helicopter nose pointed at four different azimuth angles relative to the wind. Sikorsky’s report on the tests (Reference 10) states that the test data “correlated well” to its predicted hover performance for the S-61A based on the NVH-3A testing. Note in Figure 6 that the prediction line passes through the upper part of the scatter band at the higher C_T values, and that all the points at the higher C_T s where the helicopter nose was pointed into the wind lie below the prediction line.

In its own report on the flight tests with N3173U (Reference 11), CHI states that

An unconventional test technique was selected by SAC where each loading condition [was] evaluated at four relative wind angles (0°, 90°, 180°, and 270°). The standard technique is to conduct hover tests at one azimuth, 0° (nose into the wind).

A large number of data points were generated during the three days in which conditions were satisfactory for testing (ambient winds less than 3 knots). The use of all azimuth data tends to produce an apparent significant increase in power, even though the wind is less than 3 knots It can be seen that generally, the nose into the wind data indicates the lowest power. Restricting consideration to a comparison of nose into the wind data from this test program, using the data set recorded and reduced by SAC, excellent agreement with Carson long body data ... is shown [The Carson long body data, i.e., CHI-1000-1 / RFMS #8 data] were of course taken by the standard method of hover testing with the aircraft nose into the wind.

Both CHI and SAC agree that wind effects during hover testing can be “significant.” As noted above, SAC’s prediction of the S-61A performance is based on NVH-3A data, adjusted to account for configuration differences between the NVH-3A and S-61A. To help minimize errors due to wind effects, SAC collected the baseline NVH-3A data at four wind azimuth angles, so that data points that may contain a performance decrement due to a tailwind or crosswind were collected, as well as those that may contain a performance benefit due to a headwind. The baseline NVH-3A performance was then defined by fitting a physics-based C_P - C_T curve shape through all the collected data. The volume of data collected during the N3173U “spot check” tests was insufficient to construct (reliably) a similar physics-based C_P - C_T curve fit.

CHI’s prediction of the S-61N performance is based only on data collected with the helicopter nose pointed into the wind, and hence do not include a possible performance decrement due to an adverse wind azimuth. It should be noted that CHI’s approach is consistent with industry practice and with guidance provided by the FAA in Advisory Circular AC-29C, *Certification of Transport Category Rotorcraft*, which states only that “to obtain consistent data, the wind velocity should be 3 knots or less. Large rotorcraft with high downwash velocities may tolerate higher wind velocities.”¹⁴ The AC does not mention hover testing at different azimuth angles, though FAA engineers stated in conversations with NTSB staff that testing at different azimuth angles would also be acceptable, since it would produce more conservative results.

Figure 7 shows a plot of power required vs. thrust (or weight) at the accident conditions (6106 ft pressure altitude and 23° C), for a range of thrust values near the accident weight, based on several C_P - C_T data sources. The C_P - C_T values from which the thrust and power values were computed are shown on the outer set of axes. The heavy magenta line in Figure 7 is SAC’s performance prediction for the CMRB-equipped S-61A, and the thin magenta lines depict the limits of the flight test data scatter observed in Figure 6. Note that at 19000 lb. thrust, the width of the scatter band is about 700 lb., or about 3.7% of the total thrust. Note also that the scatter band envelopes all the data plotted in the Figure.

SAC also predicted the hover performance of the S-61N model (with the “long body” fuselage) based on the USN NVH-3A and S-61A flight tests. These predictions show similar performance to the S-61A helicopter, but with an approximately 150 lb. degradation due to the increased aerodynamic download on the longer fuselage (see Figure 7). This prediction does not include the effect of the Fire King water tank, which SAC estimates would reduce the HOGE capability by about 100 lb. at the accident conditions (see Appendix A).

In addition to SAC’s performance predictions for the CMRB-equipped S-61A and S-61N, Figure 7 shows the performance for the S-61N with CMRB based on an NTSB curve-fit through the C_P - C_T flight test data published in CHI report CHI-1000-1 (Reference 8). The data documented in CHI-1000-1 was obtained by CHI during flight testing conducted in 2006, and is the basis of the HOGE performance published in CHI RFMS #8. The NTSB curve fit of the C_P - C_T data results in HOGE values that agree well with RFMS #8 at the accident conditions (6106 ft pressure altitude and 23° C). Note that if the CHI-1000-1 data were shifted to the right by approximately 150 lb. to account for the differences between an S-61A and an S-61N, the shifted line (shown as the black dash-dot line in Figure 7), representing S-61A performance, would lie slightly outside the scatter band of the data obtained with S-61A N3173U.

¹⁴ Reference 12, p. B-28 (AC 29.49(b)(3)).

Reference 11 notes that the tests documented in CHI-1000-1 were conducted with the helicopter nose pointed into the wind. These tests will therefore not reflect any performance decrement due to an adverse wind azimuth. Given the 700 lb. width of the scatter band in Figure 7, this decrement can be significant, even when measured surface winds are less than 3 knots. The CHI-1000-1 data are incorporated into RFMS #8 as the “zero wind” HOGE capability.

Results of a CHI-sponsored flight test of a S-61N equipped with CHI CMRBs

Figure 7 also shows two points labeled “Whipple flight test hover.” These points are computed based on the results of a separate flight test conducted by Whipple Aviation Services on behalf of CHI in November 2009, using a VIH Aviation Group / Cougar Helicopters S-61N equipped with CHI CMRBs (see Reference 9). The test helicopter was also equipped with an adjustable-load, 700 gallon “Fast” water bucket with a 200 ft. long-line for loading water to adjust the weight carried by the helicopter. The helicopter was not equipped with the Fire King tank.

The Whipple test was intended as a simple check of hover and climb capability at weights and conditions similar to those of the accident takeoff. Consequently, certain equipment and procedures used by SAC for hover performance flight tests were not available for the Whipple test. Specifically,

- There was no on-board instrumentation system with which to record data. Consequently, the aircraft flight instruments were used to manually record values of torque, N_R , and airspeed.
- There was no weather balloon or anemometer package with which to monitor winds at the test altitude. The aircraft GPS and airspeed indicator were used to maintain zero speed over the ground. Winds at altitude were assumed to be close to zero based on observed light winds at the surface; per Reference 9,

The aircraft airspeed indicator and the “glassy calm” lake were used to cross-reference the wind speed/direction while in the testing hovers. During the entire test period, the lake surface remained “glassy calm” which was desirable for flight-testing purposes.

However, as noted above and in Figure 5, calm winds at the surface do not necessarily ensure calm winds aloft.

- While several flight conditions are documented in Reference 9, only two steady-state hover points (with corresponding torque and N_R readings) could be identified. These two points are listed in Table 2. The C_P and C_T values obtained from these points, and the corresponding dimensional power and thrust values at the accident conditions (which are plotted in Figure 7), are also shown.

Hover Test Point	Weight (lb)	Density altitude (ft)	N_R (%)	Torque per engine (%)	Total power (HP)	C_T	C_P	Thrust at accident conditions (lb)	Power at accident conditions (HP)
Flight 1	19103	8673	103	94	2343	0.007502	0.0007456	19231	2357
Flight 2	18643	8490	103	92	2172	0.007283	0.0007258	18669	2294

Table 2. C_P and C_T computed from Whipple flight test points, and corresponding thrust and power at accident conditions (6106 ft pressure altitude, 23° C).

The Whipple flight test also documented that when collective was pulled to its upper limit, the rotor drooped to and stabilized at about 94% N_R . Figure 3 indicates that on the accident takeoff, N_R decayed to about 95%, and stabilized there for about 4 seconds. In the last 3.5 seconds, N_R dropped to about 93.5%, possibly as a result of the rotor striking the tree.

Comparison of hover performance test results

As shown in Figure 3, at the accident conditions (6106 ft pressure altitude and 23° C OAT), the total power produced by the engines is about 2300 SHP. The corresponding rotor thrust (assumed to equal helicopter weight) at this power for the S-61N equipped with CHI CMRBs based on the various data sources shown in Figure 6 is shown in Table 3.

Source	Thrust at 2300 SHP (lb)	Δ from CHI-1000-1 (lb)
CHI-1000-1 report (RFMS #8)	19120 ¹⁵	0
SAC S-61N 2010 prediction	18545	-575
Whipple flight test points	18717	-403

Table 3. Thrust at 2300 SHP, 6106 ft pressure altitude, and 23° C based on available flight-test data sources.

Of note in Table 3 is that while both the Whipple and SAC thrust values at 2300 HP are significantly less than those specified in CHI-1000-1 and RFMS #8, the differences are within the 700 lb. data scatter band shown in Figure 7 for the SAC / CHI tests of the S-61A. Consequently, the three data sources are “consistent” inasmuch as the SAC / CHI test results indicate that hover thrust cannot be known to better than about 4% of the total thrust, even in winds less than 3 knots. This uncertainty in the test results indicates that both ends of the data scatter band must be considered when evaluating the possible actual performance of the helicopter for operations, or when analyzing any particular flight, such as the accident takeoff.

Note that the net thrust values shown in Table 3 do not include the effect of rotor downwash loads on the Fire King tank, which SAC estimates to be about 100 lb. Accounting for these loads would reduce the net thrust values shown in Table 3 by about 100 lb.

¹⁵ The thrust (HOGE weight) at 2300 SHP based on RFMS #8 quoted in Reference 1 is 19100 lb, which is 20 lb less than the value shown in Figure 6. This small difference is the result in uncertainty / limits of precision in reading the RFMS charts, and in fairing a line through the scatter in the C_P - C_T data presented in CHI-1000-1.

HOGGE weights based on flight test results and accounting for the Fire King tank

The hover performance flight tests described above provide data from which C_P and C_T values can be computed. These in turn can be used to compute the net thrust (equivalent to the HOGGE weight) at a given power and density altitude. Hence, the flight test data can be used to re-compute the HOGGE weights for the three takeoffs from H44 presented in Reference 1.

Table 4 shows the results of these calculations, using the three flight test data sources described in the previous section: The CHI-1000-1 report (which is approximately equivalent to CHI RFMS #8), the SAC S-61N predictions based on the USN NVH-3A and CHI S-61A tests, and the Whipple test points. In addition, the HOGGE weights shown in Table 4 account for the 100 lb. download on the Fire King tank, which is not accounted for in RFMS #8 or the HOGGE weights presented in Reference 1, which are based on RFMS #8.

Table 4 also presents the difference between the computed HOGGE weights and the helicopter gross weight (GW) for each takeoff. Note that these margins are negative for the first and third takeoffs, if the HOGGE weights are computed using the SAC predictions or Whipple data.

Takeoff identifier:	First takeoff from H44			
Pressure altitude, ft.:	6106			
Temperature , °C:	29			
Gross weight (GW), lb.:	18368			
Power, SHP:	2224			
$C_P @ 103\% N_R$:	0.00071788			
<i>Flight test data source</i>	$C_T @ 103\% N_R$	<i>Thrust, lb.</i>	<i>HOG E weight (w/ Fire King tank), lb.</i>	<i>HOG E – GW, lb.</i>
CHI-1000-1 report (RFMS #8)	0.0073956	18581	18481	113
SAC S-61N 2010 prediction	0.0071703	18015	17915	-453
Whipple flight test points	n/a	n/a	n/a	n/a
Takeoff identifier:	Second takeoff from H44			
Pressure altitude, ft.:	6106			
Temperature , °C:	27			
Gross weight (GW), lb.:	18001			
Power, SHP:	2244			
$C_P @ 103\% N_R$:	0.00071955			
<i>Flight test data source</i>	$C_T @ 103\% N_R$	<i>Thrust, lb.</i>	<i>HOG E weight (w/ Fire King tank), lb.</i>	<i>HOG E – GW, lb.</i>
CHI-1000-1 report (RFMS #8)	0.0074073	18734	18634	633
SAC S-61N 2010 prediction	0.0071828	18166	18066	65
Whipple flight test points	n/a	n/a	n/a	n/a
Takeoff identifier:	Third takeoff from H44 (accident takeoff), 20° C			
Pressure altitude, ft.:	6106			
Temperature , °C:	20			
Gross weight (GW), lb.:	19008			
Power, SHP:	2327			
$C_P @ 103\% N_R$:	0.00072876			
<i>Flight test data source</i>	$C_T @ 103\% N_R$	<i>Thrust, lb.</i>	<i>HOG E weight (w/ Fire King tank), lb.</i>	<i>HOG E – GW, lb.</i>
CHI-1000-1 report (RFMS #8)	0.0074657	19333	19233	225
SAC S-61N 2010 prediction	0.007242	18753	18653	-355
Whipple flight test points	0.0073145	18941	18841	-167
Takeoff identifier:	Third takeoff from H44 (accident takeoff), 23° C			
Pressure altitude, ft.:	6106			
Temperature , °C:	23			
Gross weight (GW), lb.:	19008			
Power, SHP:	2300			
$C_P @ 103\% N_R$:	0.00072767			
<i>Flight test data source</i>	$C_T @ 103\% N_R$	<i>Thrust, lb.</i>	<i>HOG E weight (w/ Fire King tank), lb.</i>	<i>HOG E – GW, lb.</i>
CHI-1000-1 report (RFMS #8)	0.0074593	19120	19020	12
SAC S-61N 2010 prediction	0.0072349	18545	18445	-563
Whipple flight test points	0.007302	18717	18617	-391

Table 4. HOG E weights and margins for the three takeoffs from H44, based on available flight test data sources, and accounting for 100 lb of download on the Fire King water tank. The flight conditions for takeoffs #1 and #2 from H44 are out of the range of the available Whipple flight test data.

III. GenHel simulation results

The GenHel simulation described in Section D-I was used to compute the approximate flight path of the helicopter during the accident takeoff, for each of the following power-required conditions:

- a. Power required performance at an outside air temperature (OAT) of 23° C, as defined in the CHI Rotorcraft Flight Manual Supplement (RFMS) #8;
- b. Power required performance at an OAT of 20° C, as defined in the CHI RFMS #8;
- c. Power required performance at an OAT of 23° C, based on the SAC / USN flight tests of the USN NVH-3A and the SAC / CHI flight tests of the CHI S-61A;
- d. Power required performance at an OAT of 20° C, based on the flight tests of the USN NVH-3A and CHI S-61A.

All simulations use a helicopter gross weight of 19,008 lb. and calm winds. The collective control is driven so as to achieve a target main rotor torque that is based on the total engine torque plotted in Figure 4b. The cyclic control is driven so as to fly the helicopter to the location of the tree strike (about 195 ft. from the takeoff location) in about 30 seconds, which is the approximate time between the point where the engines reached topping, and the end of the CVR recording. In all the simulations, the helicopter is assumed to lift off and hover in ground effect at a wheel height of about 20 ft. before accelerating forward towards the tree.

The simulation results are shown in Figures 8a-8d and 9a-9d. For each of the four conditions considered, Figures 8a-8d show time-histories of the target and achieved main rotor torque, collective control deflection, and distance travelled. Figures 9a-9d plot the altitude of the helicopter rotor hub and main gear wheels against distance travelled, and also depict the sloping terrain of the mountaintop, the location of the first tree that was struck, and the height of the rotor strike mark on the tree.

Figures 8a-8d indicate that the main rotor torque computed by the simulation is oscillatory, reflecting the dynamics of the rotor. Note that the collective control is allowed to increase above the 100% position in order to achieve the “target” main rotor torque. The peaks of the torque oscillations are very close to the target torque, which represents the capability limits of the engine.

Figures 9a-9b show that when the simulation power-required performance is based on RFMS #8, the helicopter can climb, with the wheels clearing the tree by about 40 ft. for the 23° C condition, and by about 70 ft. for the 20° C condition. These results are consistent with Table 4, which shows a positive HOGE margin for both these conditions.

Figures 9c-9d show that when the simulation power-required performance is based on the SAC / USN data, the helicopter will not clear the tree at either the 23° C or 20° C condition. At an OAT of 23° C, the rotor hub impacts the tree about 6 ft. below the actual tree strike. At 20° C, the rotor hub impacts the tree about 4 ft. above the actual tree strike. These results are consistent with Table 4, which shows a negative HOGE margin for both these conditions.

E. CONCLUSIONS

The HOGE weights of the S-61N helicopter equipped with Carson / Ducommun CMRBs, computed using hover-performance flight-test data generated by both SAC / USN and Whipple Aviation Services, are significantly lower than the HOGE weights computed using hover-performance flight-test data documented in the CHI-1000-1 report and in the CHI RFMS #8. Specifically, at the accident conditions (6106 ft. pressure altitude and 23° C), the SAC / USN data predicts a HOGE capability 575 lb. less than that predicted by the CHI-1000-1 data. The Whipple data predicts a HOGE capability 403 lb. less than that predicted by the CHI-1000-1 data.

These differences are within the 700 lb. data scatter band for the SAC / CHI tests of the S-61A. Consequently, the three flight test data sources are “consistent” inasmuch as the SAC / CHI test results indicate that hover thrust cannot be known to better than about 4% of the total thrust, even in winds less than 3 knots. This uncertainty in the test results indicates that both ends of the data scatter band must be considered when evaluating the possible actual performance of the helicopter for operations, or when analyzing any particular flight, such as the accident takeoff.

The HOGE weights presented in the Hover Study (Reference 1) do not include an approximately 100 lb. download force resulting from rotor wash on the Fire King tank, which was installed on the accident helicopter, but was not installed on the helicopters that were used for the tests that resulted in the CHI-1000-1 report and RFMS #8. The HOGE margin (i.e., the difference between the HOGE weight and the helicopter gross weight) for the accident takeoff, including the effect of the Fire King tank, is shown in Table 4 for various performance bases and for outside air temperatures of 20° C and 23° C. The margin is negative if the HOGE weight is computed using either the SAC / USN data or Whipple data, ranging from -563 lb. at 23° C using the SAC / USN data, to -167 lb. at 20° C using the Whipple data. If the CHI-1000-1 / RFMS #8 data is used, the margin is +225 lb. at 20° C, and +12 lb. at 23° C.

GenHel simulations used to compute the approximate flight path of the helicopter during the accident takeoff, for various combinations of HOGE capabilities and air temperatures, indicate that the helicopter will clear a 55 ft.-high tree if the power required performance based on RFMS #8 is used, but will not clear the tree if the power required performance based on the SAC / USN flight tests is used. The simulations based on the SAC / USN data result in the rotor striking the tree within 6 ft. of the actual first tree-strike location measured at the accident site.

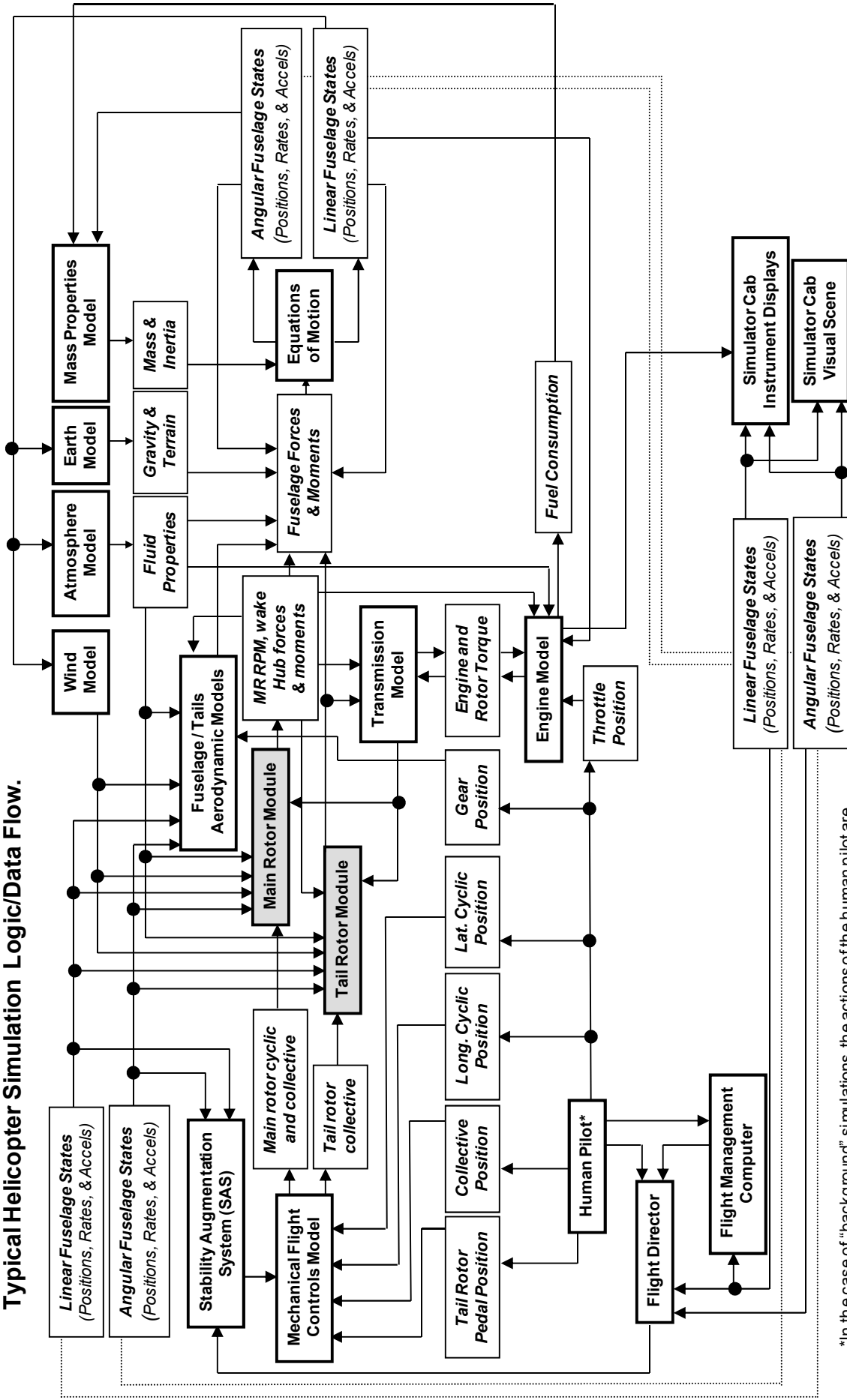
John O’Callaghan
National Resource Specialist – Aircraft Performance
Office of Research and Engineering

F. REFERENCES

1. National Transportation Safety Board, Office of Research and Engineering, *Hover Study, Errata #1, Sikorsky S-61N, Weaverville, CA, August 5, 2008*, NTSB Accident Number LAX08PA259, (Washington, DC: NTSB, March 26, 2010). (Contact NTSB at pubinq@ntsb.gov).
2. National Transportation Safety Board, Office of Research and Engineering, *Hover Study, Addendum #1, Sikorsky S-61N, Weaverville, CA, August 5, 2008*, NTSB Accident Number LAX08PA259, (Washington, DC: NTSB, April 13, 2010). (Contact NTSB at pubinq@ntsb.gov).
3. National Transportation Safety Board, Office of Research and Engineering, *Sound Spectrum Study Cockpit Voice Recorder, Sikorsky S-61N, Weaverville, CA, August 5, 2008*, NTSB Accident Number LAX08PA259, (Washington, DC: NTSB, May 1, 2009). (Contact NTSB at pubinq@ntsb.gov). See also Errata to the *Sound Spectrum Study Cockpit Voice Recorder*, dated March 25, 2010.
4. National Transportation Safety Board, Office of Research and Engineering, *Cockpit Voice Recorder Group Chairman's Factual Report, Sikorsky S-61N, Weaverville, CA, August 5, 2008*, NTSB Accident Number LAX08PA259, (Washington, DC: NTSB, August 17, 2009). (Contact NTSB at pubinq@ntsb.gov).
5. J. J. Howlett, *NASA Contractor Report 166309: UH-60A Black Hawk Engineering Simulation Program: Volume I – Mathematical Model*. Ames Research Center Contract NAS2-10626, December 1981.
6. J. J. Howlett, *NASA Contractor Report 166310: UH-60A Black Hawk Engineering Simulation Program: Volume II – Background Report*. Ames Research Center Contract NAS2-10626. General release December 30, 1988.
7. National Transportation Safety Board, Office of Aviation Safety, *Airworthiness Group Chairman's Factual Report, Sikorsky S-61N, Weaverville, CA, August 5, 2008*, NTSB Accident Number LAX08PA259, (Washington, DC: NTSB, September 10, 2009). (Contact NTSB at pubinq@ntsb.gov).
8. Carson Helicopters, Inc., *Development of Charts for Rotorcraft Flight Manual Supplement No. 6 (Revised)*. Report Number CHI-1000-1, Rev B, May 22, 2007.
9. Whipple Aviation Services, Inc., *Aircraft Performance Evaluation Report: Project: Performance Evaluation Test Flight, VIH Cougar Helicopters SK-61N // N261F, Reno Stead Airport, Reno, NV, 03 November 09*. Prepared for Carson Helicopters, Inc., 828 Brookside Blvd, Grants Pass, OR, 97523. Docket Item # 182 (Contact NTSB at pubinq@ntsb.gov).
10. Sikorsky Aircraft Corporation, Report # SER-612014, Appendix B, *Department of State S-61N Hover Performance Data & Charts*. Provided to NTSB on October 4, 2010. (Contact NTSB at pubinq@ntsb.gov).
11. Carson Helicopters, Inc. *S-61 Long Body Hover Performance Test Report*. Report Number CHI-61-100, prepared by H. C. Curtiss, October 19, 2010.
12. Federal Aviation Administration, Advisory Circular AC-29C Change 3, *Certification of Transport Category Rotorcraft*. U.S. Department of Transportation, Federal Aviation Administration, September 30, 2008.

FIGURES

Typical Helicopter Simulation Logic/Data Flow.



*In the case of "background" simulations, the actions of the human pilot are replaced by instructions in user defined "scenario file" computer programs.

Figure 1.

Main Rotor Module

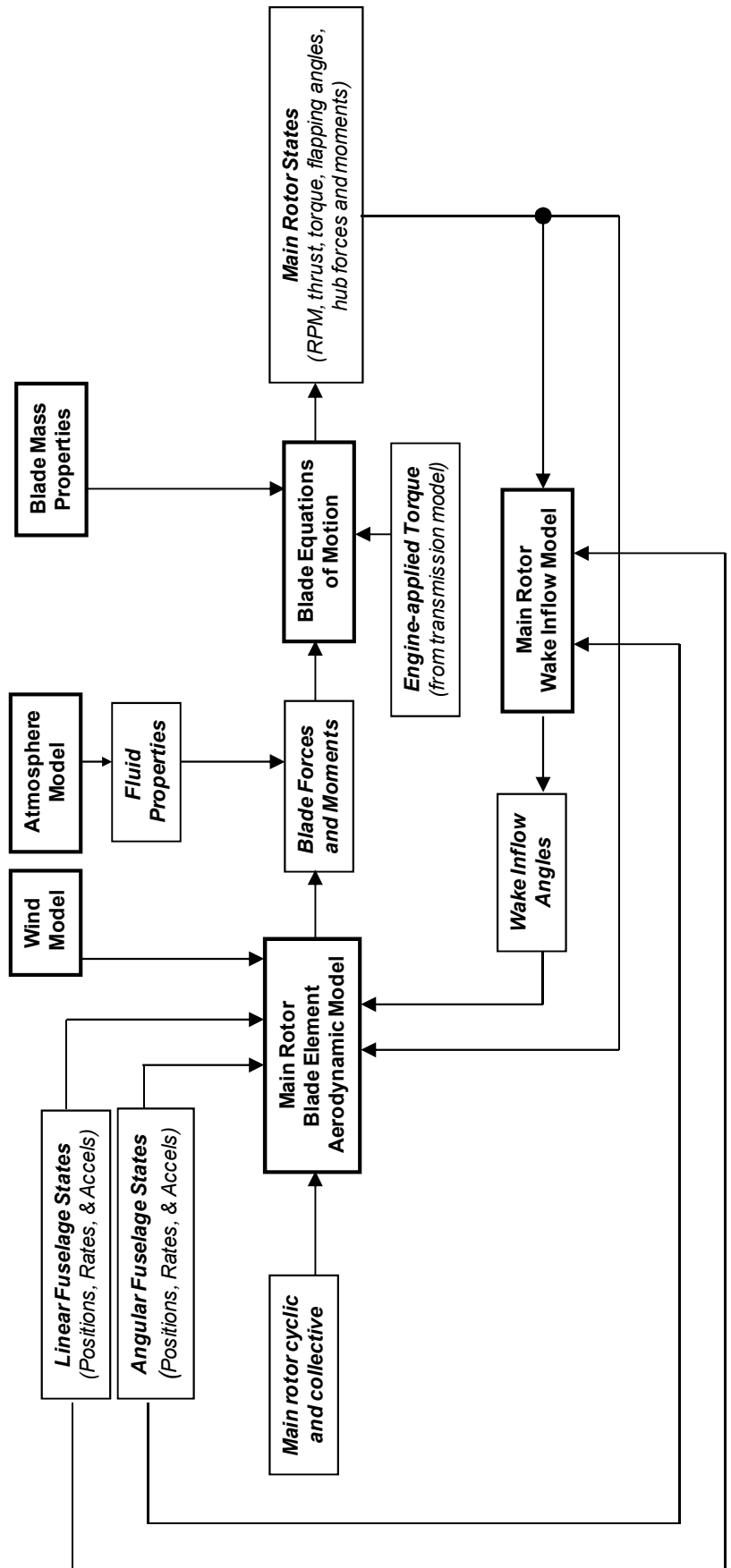


Figure 2. Logic and data flow schematic for the main rotor module within a helicopter simulation.

Engine and rotor speed, engine power, and HOGE weight vs. time H44 takeoff #3 (accident): $h_p = 6106$ ft, OAT = 23° C & 20° C, wind calm

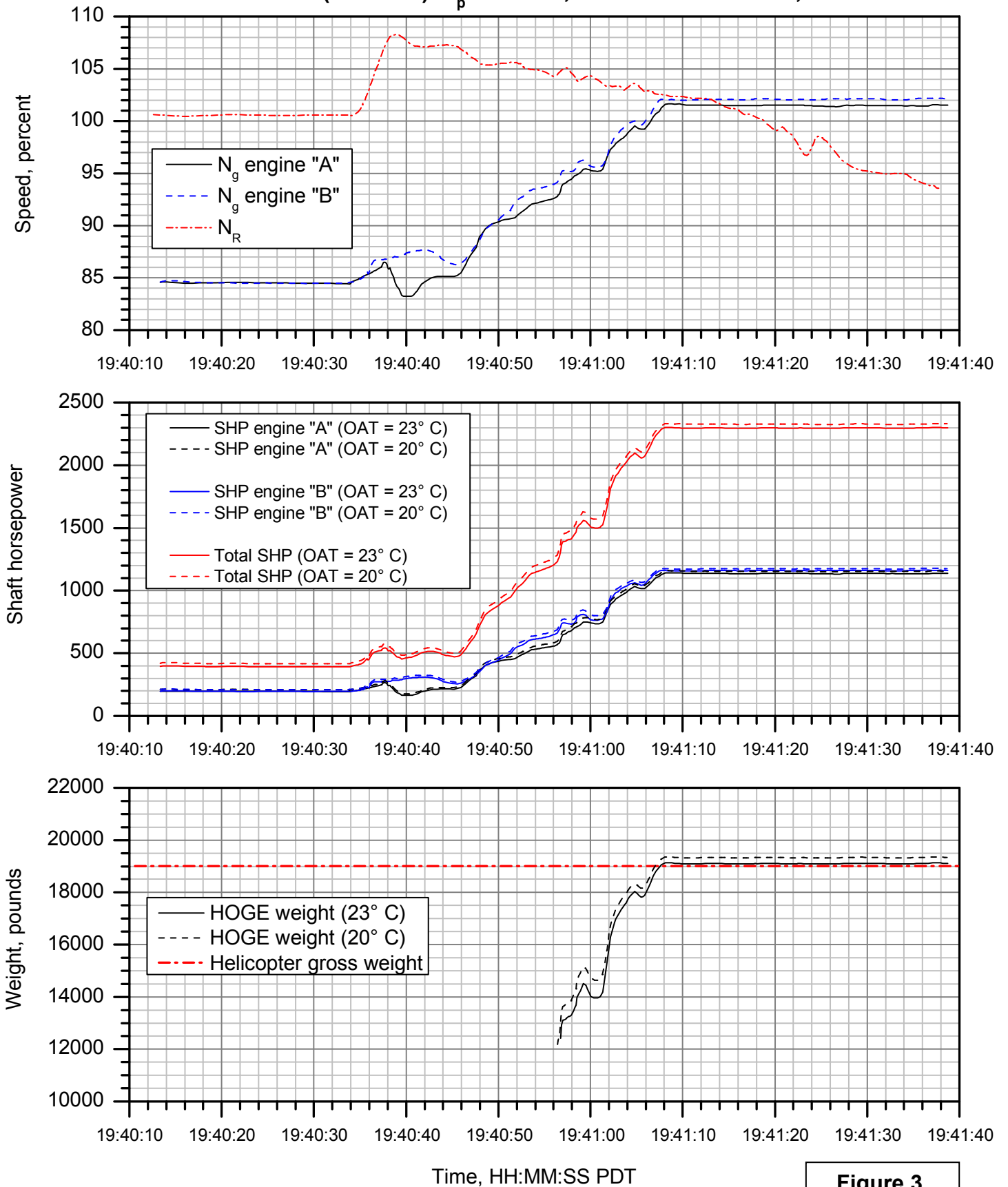
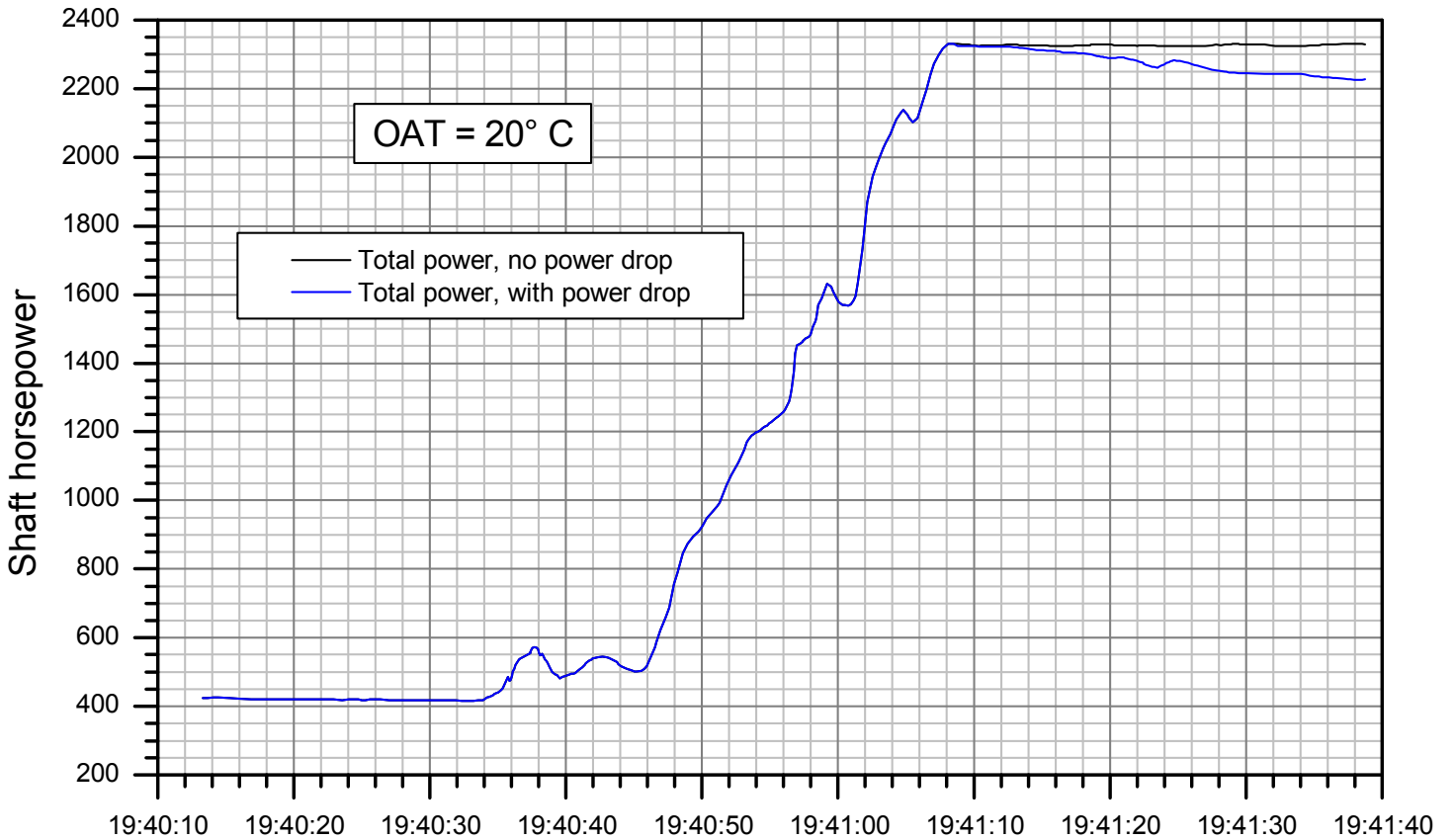
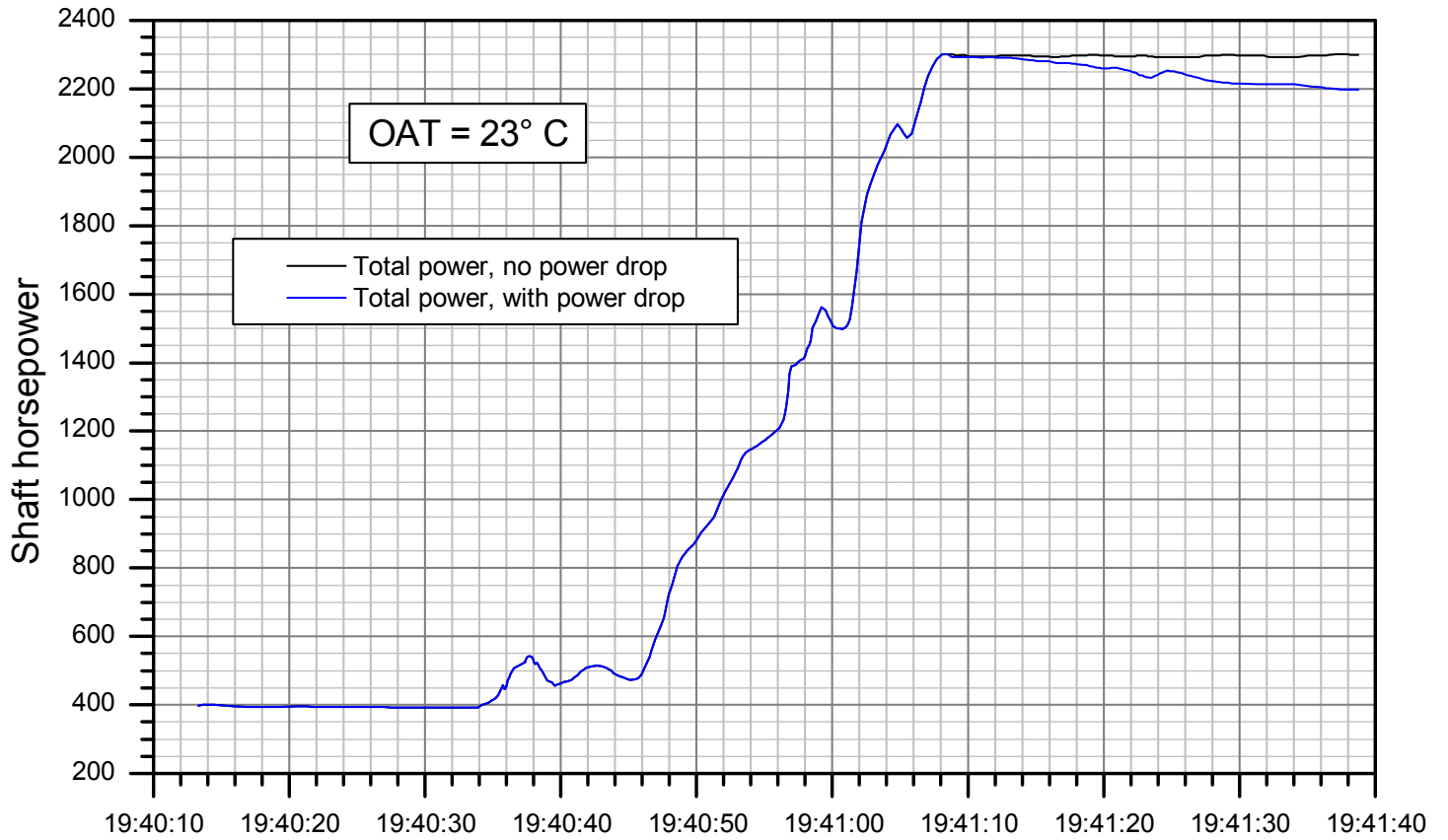


Figure 3.

Engine power vs. time, with power drop during N_R drop at topping

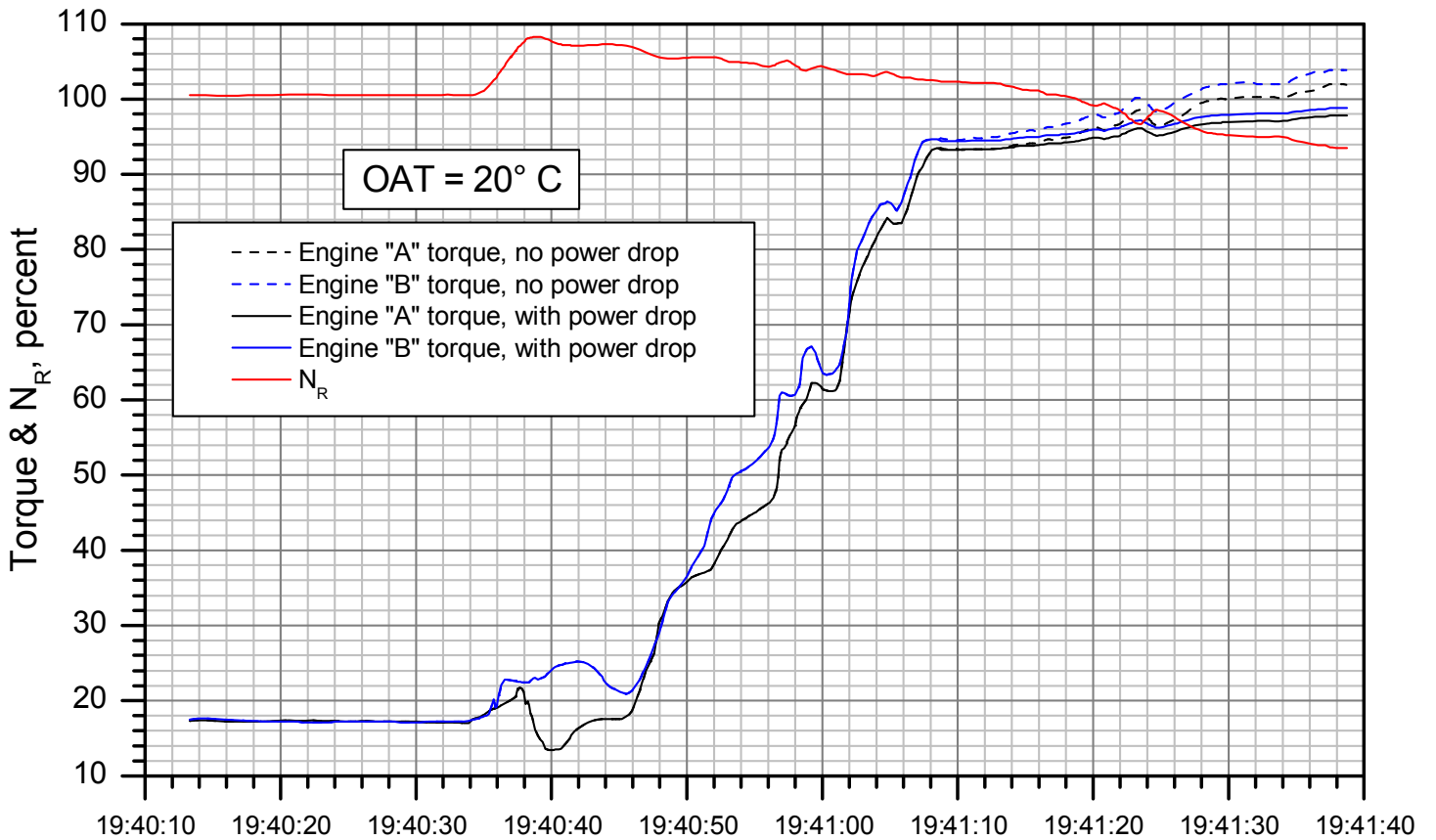
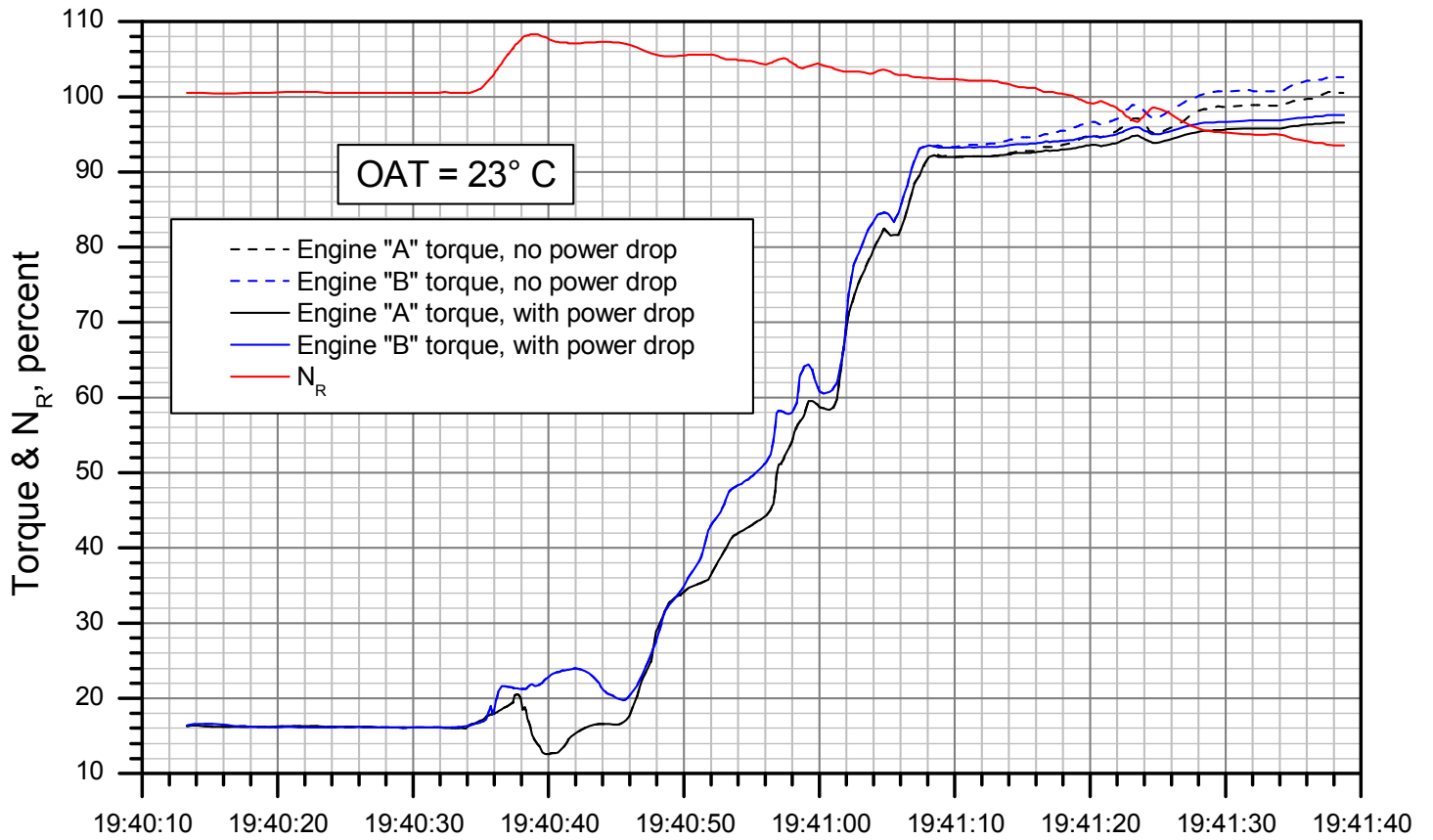
H44 takeoff #3 (accident): $h_p = 6106$ ft, OAT = 23° C & 20° C



Time, HH:MM:SS PDT

Figure 4a.

Engine torque vs. time, with power drop during N_R droop at topping
H44 takeoff #3 (accident): $h_p = 6106$ ft, OAT = 23° C & 20° C



Time, HH:MM:SS PDT

Figure 4b.



Figure 5. Image of a tethered balloon with streamers attached at various points along the tether, showing calm winds at the surface and higher winds at the balloon altitude (image provided by SAC).

OGE Hover "Spot Check" 3KTS or Less D.O.S. S-61N 173U Aircraft

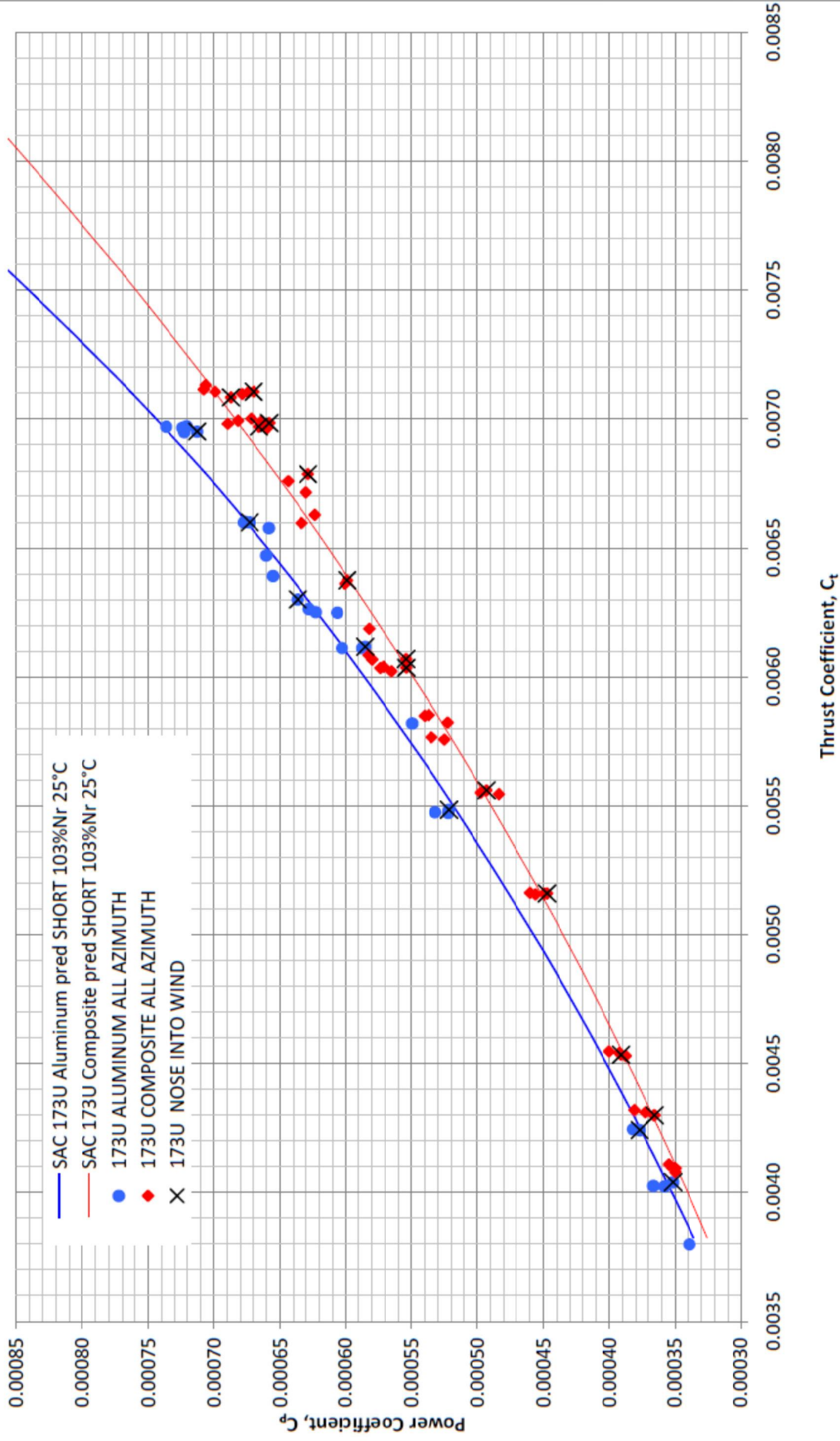


Figure 6. Plot of C_p vs. C_T based on the results of the SAC / CHI hover performance flight tests of N3173U (from Reference 10).

S-61 CMRB Power required vs. thrust: CHI-1000-1 report data (basis of RFMS #8 - long body), Whipple flight test points, and SAC 2010 S-61A (short body) and S-61N (long body) predictions based on USN VH-3A & CHI S-61A flight test data

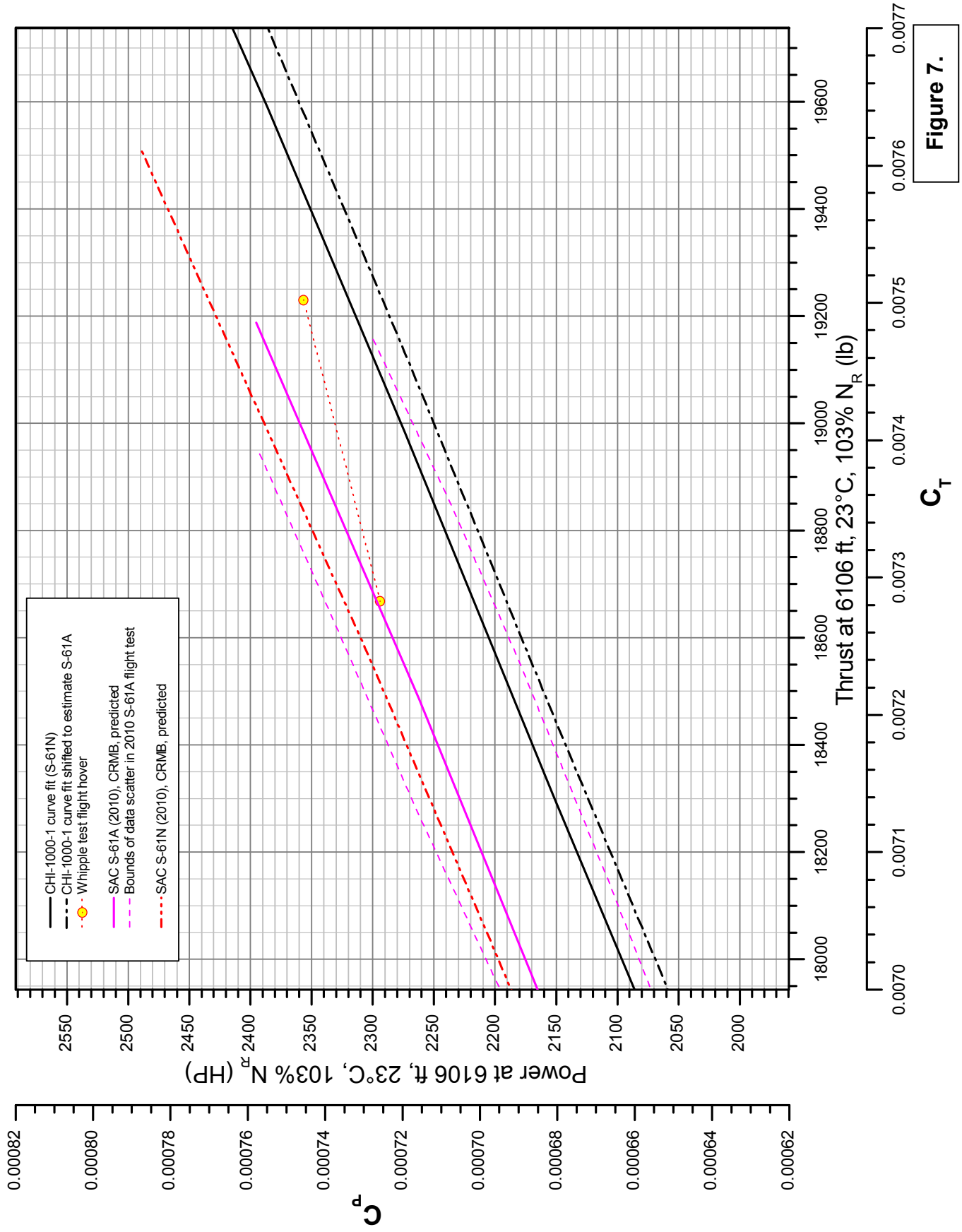


Figure 7.

GenHel simulation results, condition "a": RFMS #8 performance, 23° C Collective position, main rotor torque, and distance travelled

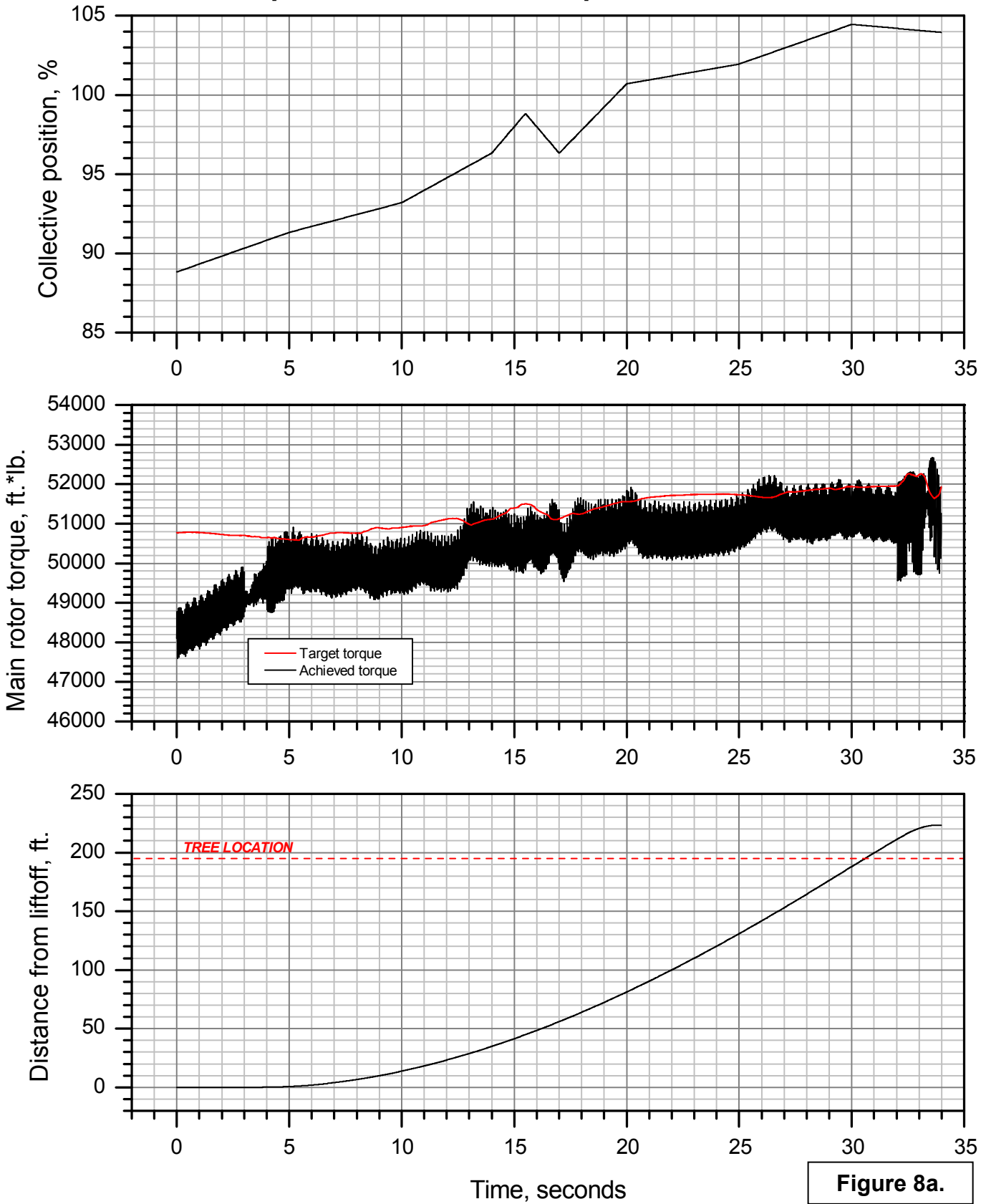


Figure 8a.

GenHel simulation results, condition "b": RFMS #8 performance, 20° C Collective position, main rotor torque, and distance travelled

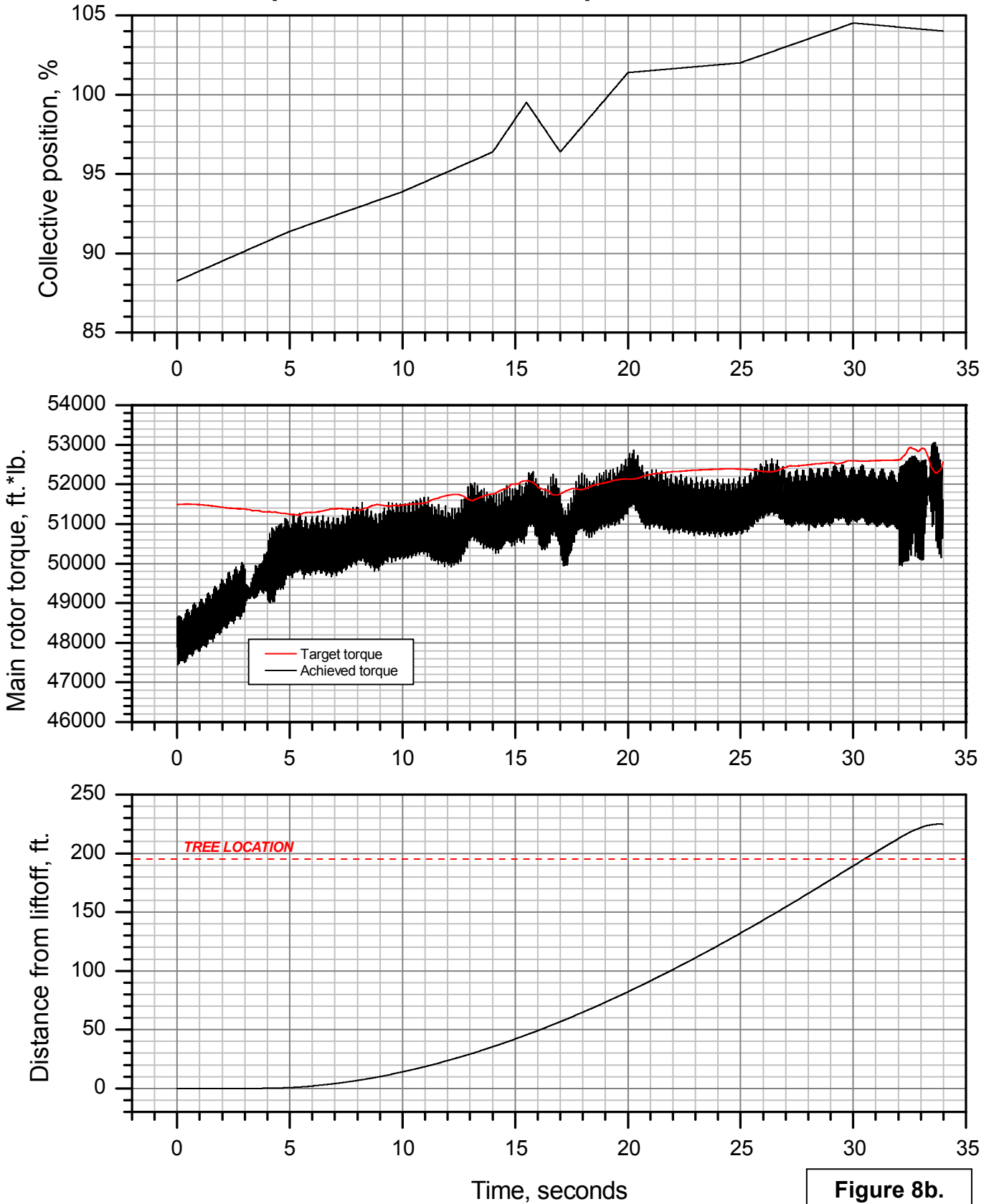


Figure 8b.

GenHel simulation results, condition "c": SAC / USN performance, 23° C Collective position, main rotor torque, and distance travelled

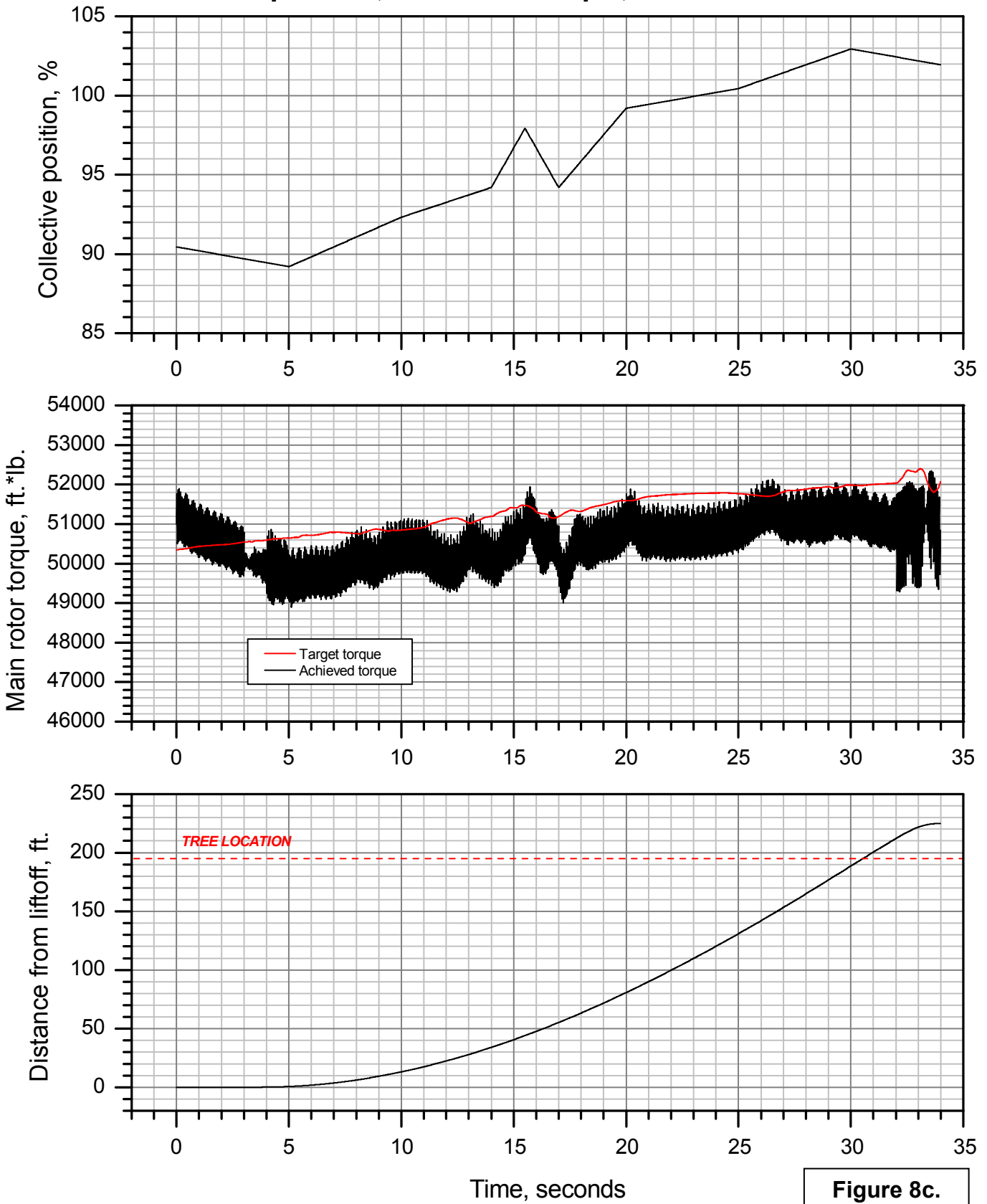


Figure 8c.

GenHel simulation results, condition "d": SAC / USN performance, 20° C Collective position, main rotor torque, and distance travelled

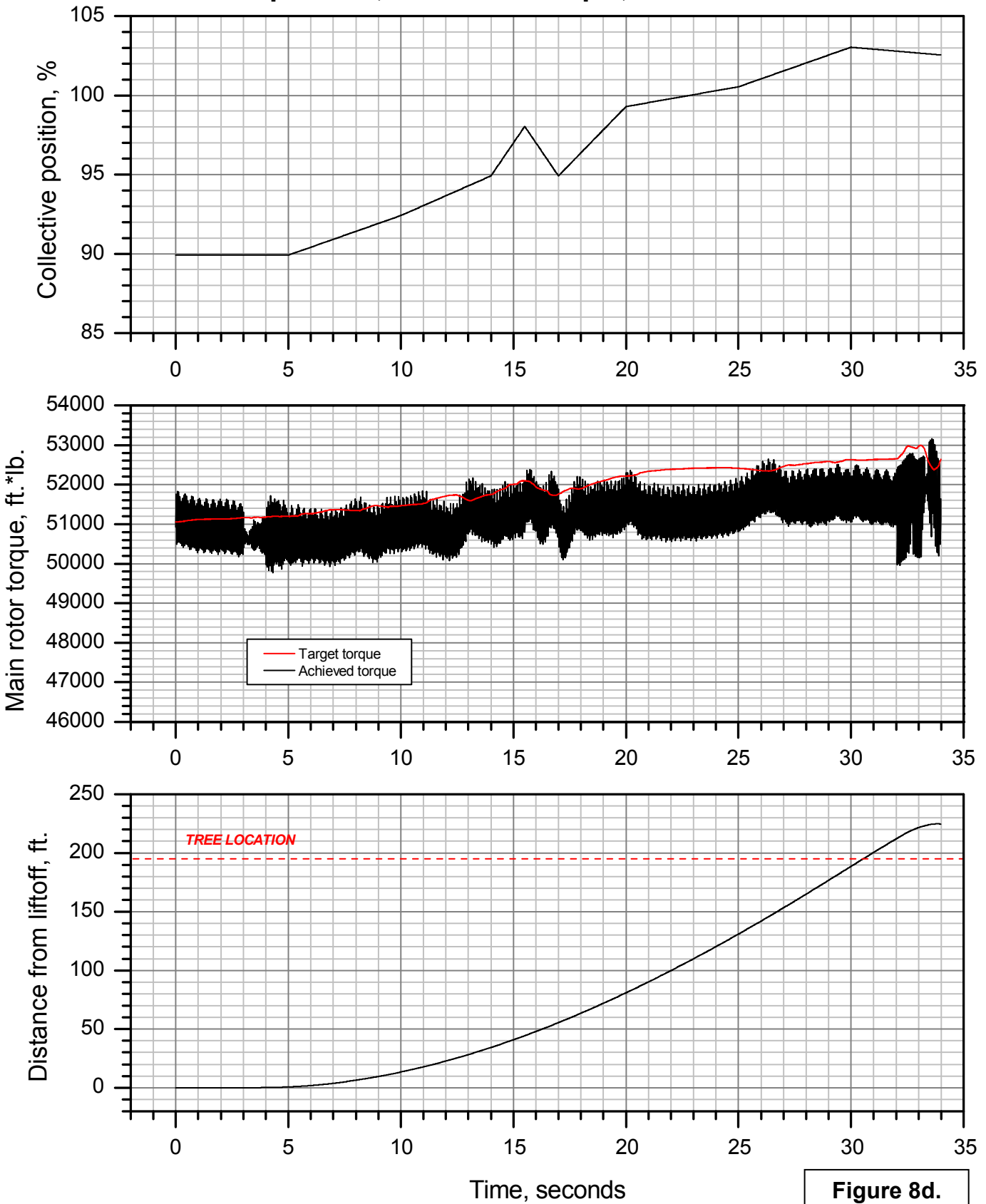


Figure 8d.

GenHel simulation results, condition "a": RFMS #8 performance, 23° C Altitude of rotor hub and wheels vs. distance travelled

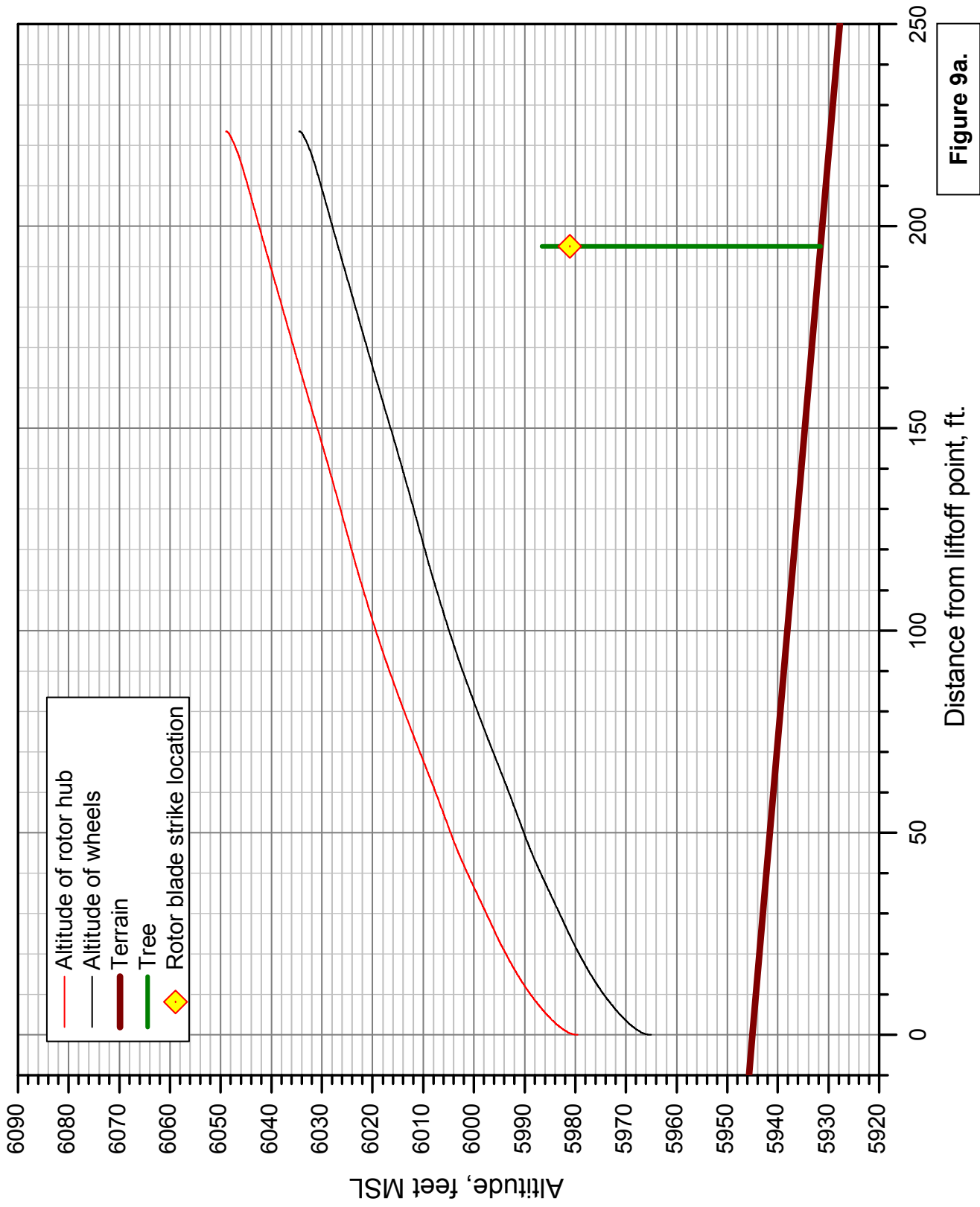


Figure 9a.

GenHel simulation results, condition "b": RFMS #8 performance, 20° C Altitude of rotor hub and wheels vs. distance travelled

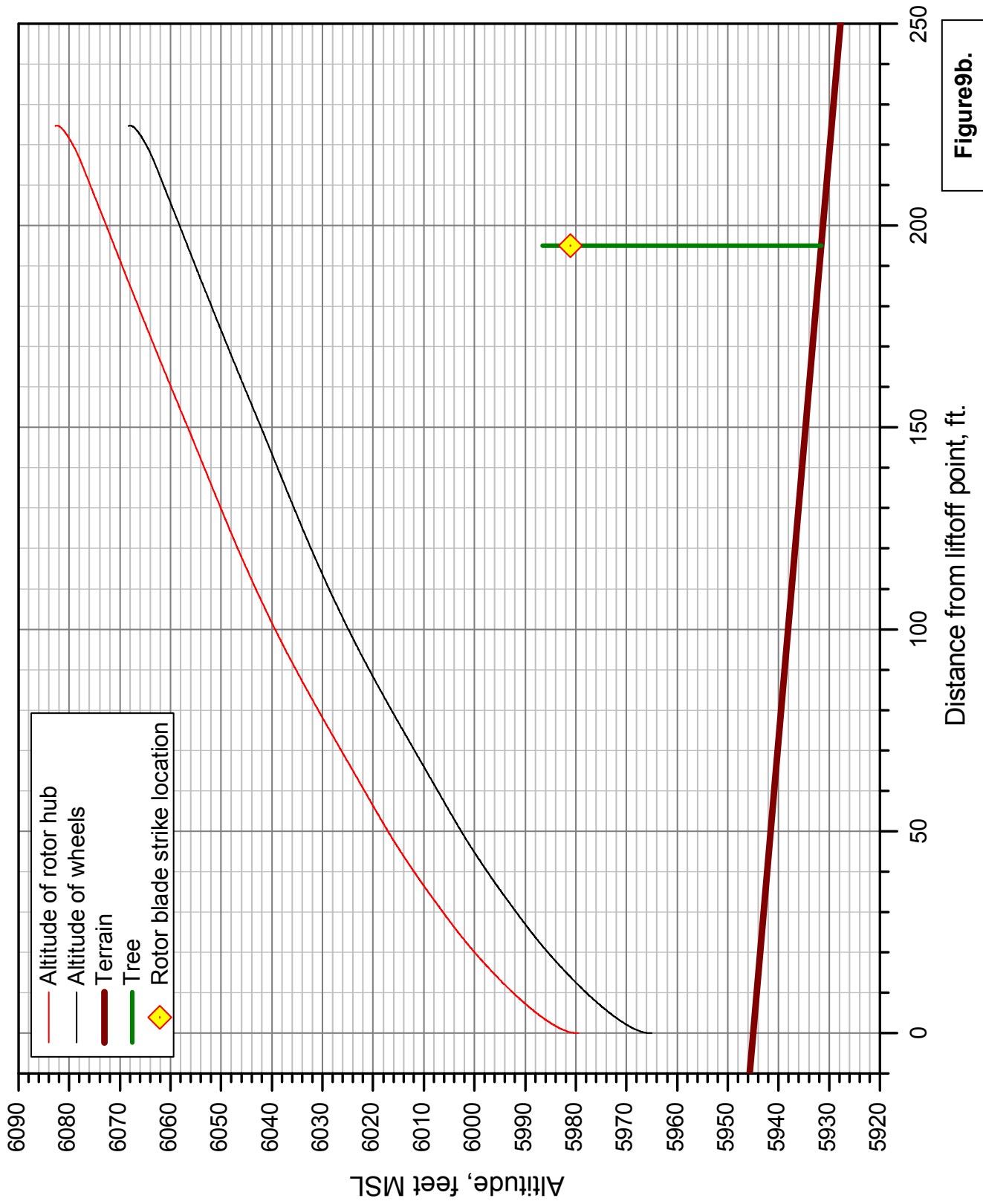


Figure9b.

GenHel simulation results, condition "c": SAC / USN performance, 23° C Altitude of rotor hub and wheels vs. distance travelled

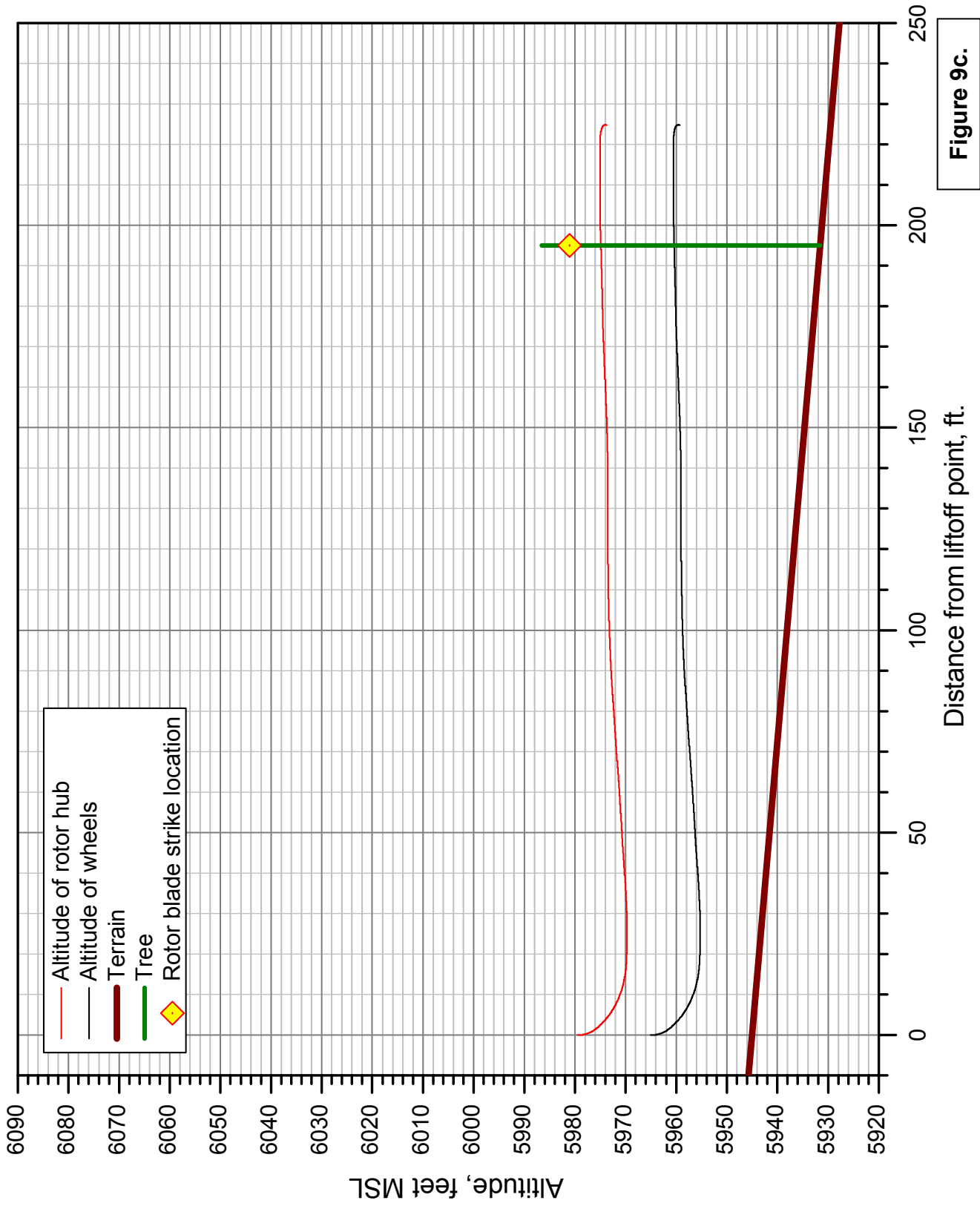
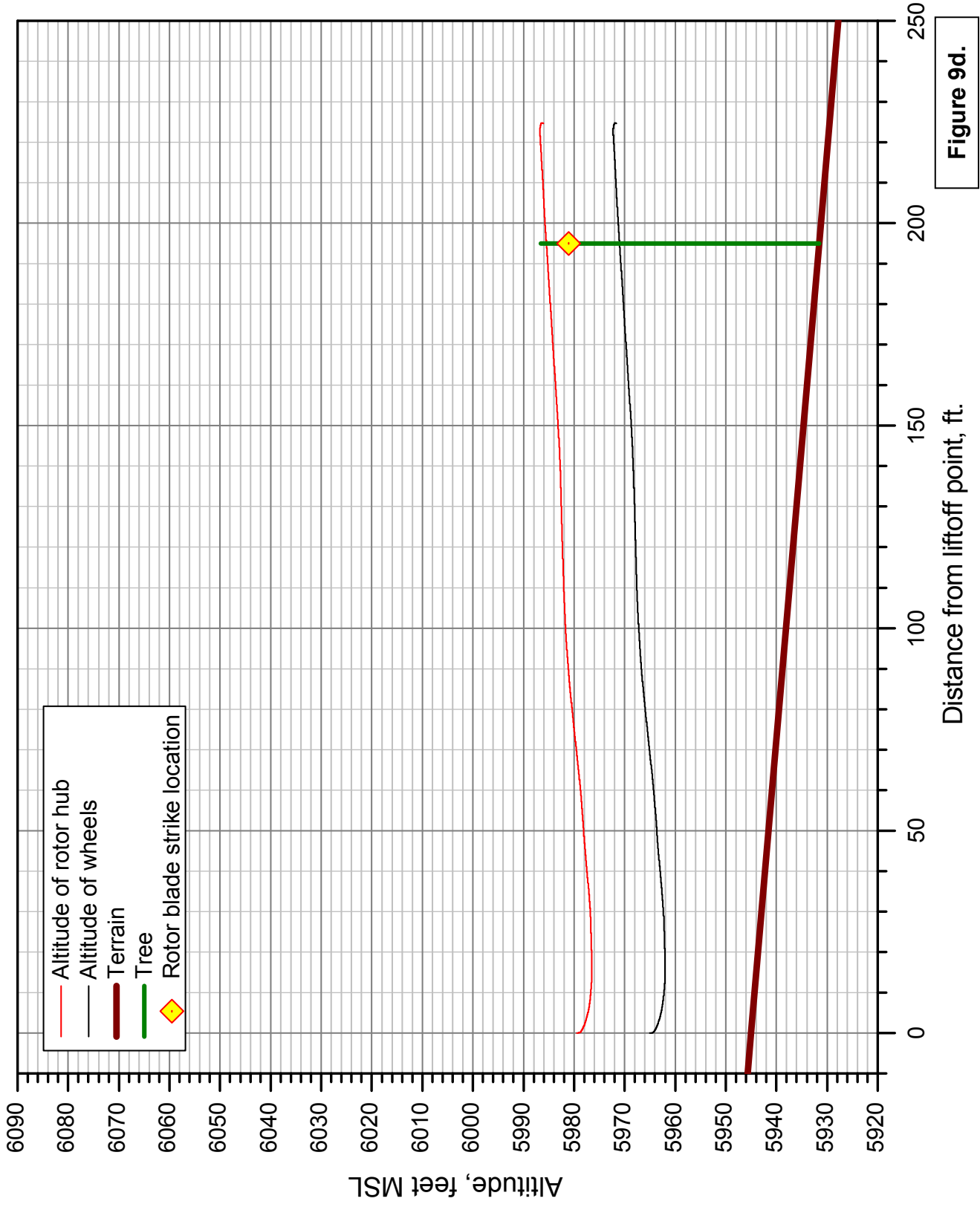


Figure 9c.

GenHel simulation results, condition "d": SAC / USN performance, 20° C

Altitude of rotor hub and wheels vs. distance travelled



APPENDIX A

Fire King Tank Download Analysis

by

Sikorsky Aircraft Company

Hover Download Analysis

April 15, 2010

May 20, 2010 Revision 1 (corrected geometry of tank 1st iteration)

August 31, 2010 Revision 2e (corrected geometry 2nd iteration)

November 3, 2010 Revision 3 (removed landing gear data)

Introduction

The method for assessing the download of the fuselage and other components at Sikorsky Aircraft is a typical strip analysis as shown in Figure 1. The area underneath the rotor is divided into a large number of annular strips. Under each strip, the area and estimated drag coefficient the item to be evaluated is provided along with the distance under the rotor. The downwash velocity on each component is calculated based on the distance from the center of rotation and the distance below the rotor. Velocities increase as radial distance increases and as the vertical distance increases. The results are updated if well instrumented flight test data are available. Note, the sketch below shows the legacy Sikorsky aluminum blades; however, the actual geometry of the Carson Composite Main Rotor Blade (CMRB) including airfoils, twist, and root cut-out was used for the analysis.

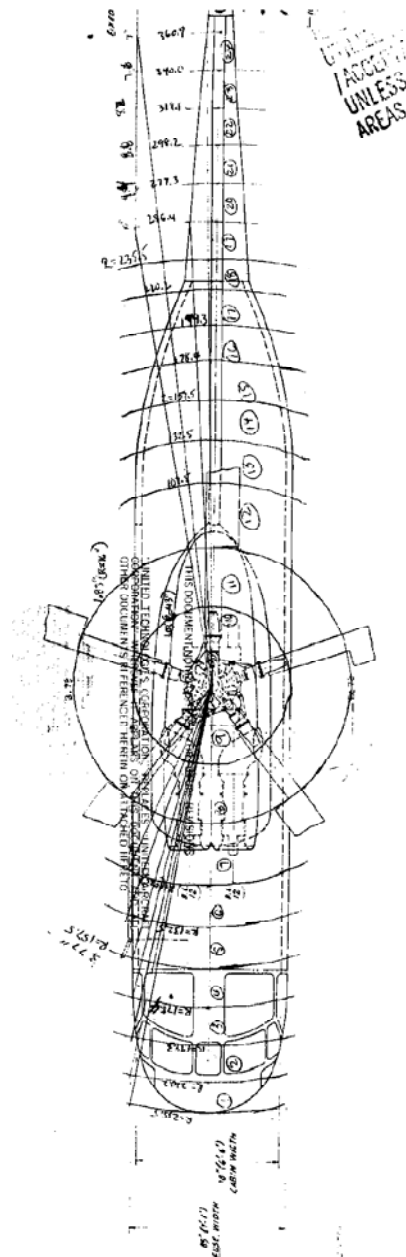


Figure 1 – Strip Analysis

Fire King Tank Download Analysis

For the initial April 2010 download estimate, no dimensioned drawing of the Fire King tank was available, but use of pictures and scaling from known dimensions allowed a reasonable estimate of the projecting area and location to be made. Note that the tank does extend beyond the limits of the fuselage as shown in Figure 2. After Sikorsky's first analysis, the NTSB supplied Sikorsky with revised tank dimensions and asked for the download analysis to be performed a second time. Carson later responded to the NTSB disputing the conclusions of the analysis. Although Carson never provided the three-view drawings that the NTSB had requested, they did provide some revised dimensions and clarified the tank's location relative to aircraft fuselage stations. The NTSB also provided Sikorsky Aircraft with additional photos supplied by another operator who uses Carson's Fire King tank. The NTSB asked Sikorsky to perform the analysis a third and final time using these new dimensions and locations.



Figure 2 – Fire King Tank

The tank was stated by Carson to be 107 inches long, extending from fuselage station (STA) 213 to STA320. The width of the tank was stated by Carson to be 130 inches. Since the basic fuselage is 85 inches wide, the tank protrudes 22.5 inches beyond each side of the fuselage. This gives a projected area of 16.72 square feet on each side or 33.44 square feet total. Since the tank has a flat top with subcritical curved sides, the drag coefficient assigned was 1.2 and the result was a predicted download of 0.54% or 103 lbs at a gross weight of 19,000 lbs. Note that this analysis remains *conservative*, because it does not account for the additional drag that is created by the various nozzles, elbows, and fittings that project out from both the front (12.5 inches) and rear (8 inches) of the tank faces. (note that Revision 1 and 2 both resulted in 0.54% and 103 lbs, using different methods of calculation)

Fire King Tank Frontal Drag

The frontal drag of the tank was estimated using the dimensions taken from scaling pictures. The bottom of the tank was assumed to be at waterline (WL) 67 with a deadrise angle of 12° to match the bottom of the fuselage. The top of the tank was estimated to be at WL106 with the end of the tank along buttlane 65.0 as noted earlier (width of 130 inches). The resulting frontal area is 17.4 square feet. The front of the tank has a flat face with a step in height in the outboard part about fuselage station 240. The drag coefficient was assessed as being 0.8 to account for the step and the fact that the front fuselage will slow the air somewhat before reaching the tank. This gives an equivalent flat plate tank frontal drag area of 13.9 square feet. Note: In order to be conservative, Sikorsky maintained the original equivalent frontal drag area of 13.44 square feet in our calculations.